AGU PUBLICATIONS

Global Biogeochemical Cycles

RESEARCH ARTICLE
10.1002/2017GB005622

Key Points:
- Simultaneous measurement of gross rates of CH_4 production and oxidation revealed complex responses of these processes to varying redox
- Heterogeneous distribution of CH_4 production and oxidation leads to smaller net CH_4 fluxes than predicted by water table position
- An emerging conceptual model based on heterogeneous redox better represents peatland CH_4 dynamics than redox strata set by the water table

Supporting Information:
- Supporting Information S1

Correspondence to:
W. H. Yang,
yangw@illinois.edu

Citation:
Yang, W. H., McNicol, G., Teh, Y. A., Estera-Molina, K., Wood, T. E., & Silver, W. L. (2017). Evaluating the classical versus an emerging conceptual model of peatland methane dynamics. *Global Biogeochemical Cycles*, *31*. https://doi.org/10.1002/2017GB005622

Received 24 JAN 2017
Accepted 26 AUG 2017
Accepted article online 30 AUG 2017

Evaluating the Classical Versus an Emerging Conceptual Model of Peatland Methane Dynamics

Wendy H. Yang[1], Gavin McNicol[2,3], Yit Arn Teh[4], Katerina Estera-Molina[2], Tana E. Wood[5], and Whendee L. Silver[2]

[1]Department of Plant Biology and Department of Geology, University of Illinois at Urbana-Champaign, Urbana, IL, USA, [2]Ecosystem Sciences Division, Department of Environmental Science, Policy, and Management, University of California, Berkeley, CA, USA, [3]Now at Department of Natural Science, University of Alaska Southeast, Juneau, AK, USA, [4]Institute of Biological and Environmental Sciences, University of Aberdeen, Aberdeen, UK, [5]USDA Forest Service, International Institute of Tropical Forestry, Rio Piedras, Puerto Rico

Abstract Methane (CH_4) is a potent greenhouse gas that is both produced and consumed in soils by microbially mediated processes sensitive to soil redox. We evaluated the classical conceptual model of peatland CH_4 dynamics—in which the water table position determines the vertical distribution of methanogenesis and methanotrophy—versus an emerging model in which methanogenesis and methanotrophy can both occur throughout the soil profile due to spatially heterogeneous redox and anaerobic CH_4 oxidation. We simultaneously measured gross CH_4 production and oxidation in situ across a microtopographical gradient in a drained temperate peatland and ex situ along the soil profile, giving us novel insight into the component fluxes of landscape-level net CH_4 fluxes. Net CH_4 fluxes varied among landforms ($p < 0.001$), ranging from 180.3 ± 81.2 mg C m^{-2} d^{-1} in drainage ditches to -0.7 ± 1.2 mg C m^{-2} d^{-1} in the highest landform. Contrary to prediction by the classical conceptual model, variability in methanogenesis alone drove the landscape-level net CH_4 flux patterns. Consistent with the emerging model, freshly collected soils from above the water table produced CH_4 within anaerobic microsites. Even in soil from beneath the water table, gross CH_4 production was best predicted by the methanogenic fraction of carbon mineralization, an index of highly reducing microsites. We measured low rates of anaerobic CH_4 oxidation, which may have been limited by relatively low in situ CH_4 concentrations in the hummock/hollow soil profile. Our study revealed complex CH_4 dynamics better represented by the emerging heterogeneous conceptual model than the classical model based on redox strata.

1. Introduction

Soils are a globally important source of methane (CH_4), a potent greenhouse gas that has increased 2.5-fold in atmospheric concentration since preindustrial times and accumulated in the atmosphere at a rate of 6 Tg CH_4 yr^{-1} from 2000 to 2009 (Ciais et al., 2013). At the same time, soils are also an important sink of CH_4, removing between 9 and 47 Tg CH_4 each year (Ciais et al., 2013). Generally, an ecosystem functions as either a source or a sink for atmospheric CH_4, with natural wetlands as the largest natural source of CH_4 and upland ecosystems as the dominant soil CH_4 sink (Ciais et al., 2013). However, peat-forming wetlands, including peat bogs, fens, and other histosols, can switch between acting as CH_4 sources or sinks depending on hydrologic conditions and water table depth. High water tables limit oxygenation and promote highly reducing conditions conducive for methanogenesis, provided that the availability of alternative electron acceptors do not give other anaerobic processes a competitive advantage (Megonigal et al., 2004). Water table drawdown can occur through management for agricultural purposes (e.g., Drexler et al., 2009; Koh et al., 2011; Maljanen et al., 2010), as a result of natural drought (e.g., Alm et al., 1999; Fenner & Freeman, 2011; Goodrich et al., 2015; Yavitt, 2013), and potentially due to climate change-induced decreases in precipitation (Li et al., 2007) or increases in evapotranspiration (Roulet et al., 1992). This can lead to oxygenation of the surface peat that can inhibit methanogenesis and support methanotrophy, causing substantial reductions in net CH_4 source strength (Goodrich et al., 2015; Hatala et al., 2012; Nykanen et al., 1995; Schrier-Uijl et al., 2010; Updegraff et al., 2001) or even a switch to net CH_4 uptake on the ecosystem scale (Langeveld et al., 1997; Roulet et al., 1993). Peatlands occur in northern, temperate, and tropical latitudes and store a large percentage of the global soil C stock that is vulnerable to mineralization under drier conditions (Limpens et al., 2008a, 2008b). In some instances, increases in methanotrophy following water table drawdown can

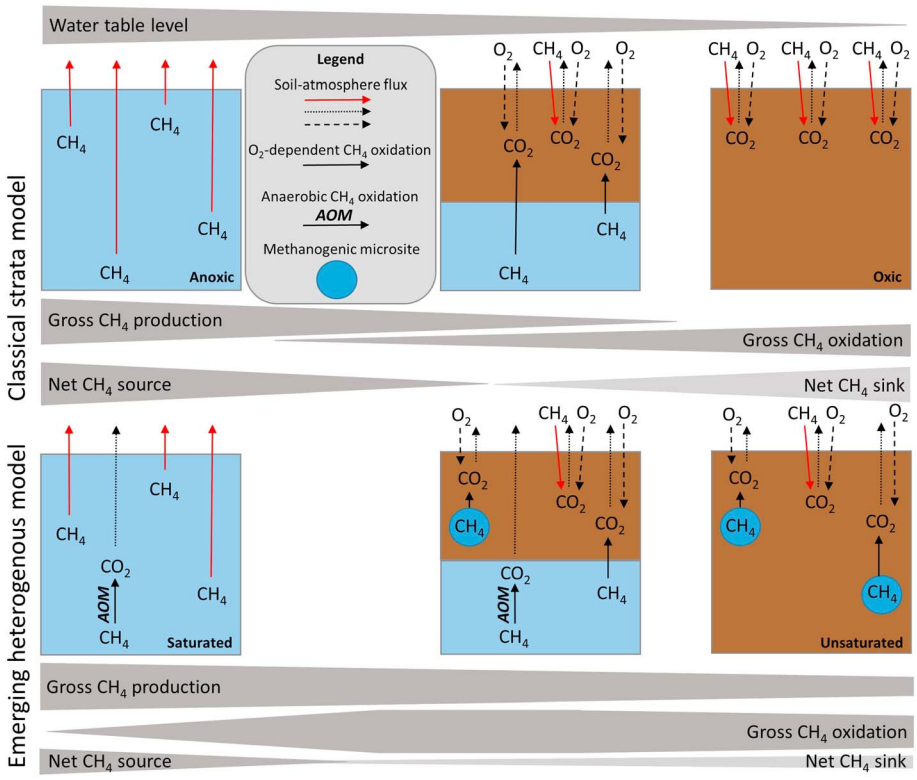

Figure 1. Pedon-scale conceptual models of water table effects on CH_4 dynamics in a peatland ecosystem. The classical strata model assumes that methanogenesis occurs in anoxic soils only beneath the water table after more energetically favorable TEAs have been depleted, and methanotrophy occurs only above the water table where O_2 diffusion into unsaturated soils can support O_2-dependent CH_4 oxidation. The emerging heterogeneous model includes methanogenesis in highly reducing microsites in unsaturated soils above the water table (where the C supply is sufficient to drive the local depletion of alternative TEAs) and anaerobic CH_4 oxidation (AOM) in saturated soils below the water table. The height of the water table and the magnitude of net CH_4 fluxes, gross CH_4 production rates, and gross CH_4 oxidation rates are indicated by the width of the gray bars.

be large enough to wholly or partially offset the global warming potential arising from enhanced peat C mineralization due to accelerated aerobic decomposition in newly oxygenated layers (Neubauer & Megonigal, 2015). A better understanding of the mechanisms controlling CH_4 production and oxidation in peatlands would allow us to better predict how net CH_4 fluxes will respond to changes in water table depth and contribute to ecosystem feedbacks to climate change.

The classical conceptual model of CH_4 dynamics posits that bulk soil redox boundaries, largely occurring along vertical profiles at the pedon scale, predict patterns in CH_4 production and oxidation (Figure 1). Fundamentally, thermodynamics and the energetics of methanogenesis and methanotrophy constrain these processes: methanogenesis can only occur under highly reducing conditions (Fetzer et al., 1993; Zinder, 1993), whereas aerobic CH_4 oxidation—which is thought to be the predominant biotic sink for CH_4 in terrestrial freshwater environments—is limited by CH_4 or oxygen (O_2) availability (Bender & Conrad, 1994; Riley et al., 2011). Therefore, according to this model, methanogenesis predominantly occurs below the water table, where limited O_2 diffusion leads to the sequential reduction of alternative terminal electron acceptors (TEAs) until methanogenesis becomes thermodynamically favorable (Lueders & Friedrich, 2000; Peters & Conrad, 1996; Yao et al., 1999). Conversely, this model predicts increased CH_4 oxidation in the unsaturated —and implicitly oxic—surface layers above the water table, with the highest CH_4 oxidation potential just above the water table where CH_4 concentrations are highest (Adamsen & King, 1993; Bender & Conrad, 1994; Happell & Chanton, 1993; Hornibrook et al., 2009; Moore & Dalva, 1993; Roulet et al., 1993; Whalen & Reeburgh, 1990). Peatlands encompass a wide range of ecosystems that differ in the degree of peat decomposition (i.e., sapric, hemic, and fibric), peat-forming vegetation (e.g., mosses, shrubs, and sedges),

and hydrology and nutrient inputs (i.e., ombrotrophic versus minerotrophic) that shape the organic matter quantity and quality, nutrient status, hydrological regimes, and microbial communities that distally regulate CH_4 dynamics. The classical conceptual model of peatland CH_4 dynamics is powerful because it captures the proximal control on CH_4 dynamics that is shared by these diverse ecosystems: water table position sets the oxic-anoxic boundary that delineates vertical zones, or strata, of methanogenesis and methanotrophy.

Contrary to this classical strata model, we now know that soil CH_4 dynamics are not so clearly regulated by bulk soil O_2 availability nor are these processes strictly depth stratified. Methanogenesis commonly occurs in anoxic microsites within unsaturated soils or drained soil layers (Sey et al., 2008; Silver et al., 1999; Teh & Silver, 2006; Teh et al., 2005; von Fischer & Hedin, 2002, 2007; Yang & Silver, 2016); methanogenesis can co-occur with other anaerobic respiration pathways when TEAs are still present in flooded soils (Knorr & Blodau, 2009); and CH_4 can be oxidized in the absence of O_2 using other TEAs such as nitrate (NO_3^-), sulfate, and organic matter (Beal et al., 2009; Blazewicz et al., 2012; Gauthier et al., 2015; Gupta et al., 2013; Raghoebarsing et al., 2006; Smemo & Yavitt, 2007, 2011; Valenzuela et al., 2017). While these mechanisms are now well described, Earth system models (ESMs) still commonly represent wetland CH_4 production as some fraction of heterotrophic respiration scaled by a function of water table position or soil moisture (Wania et al., 2013), and only one model has considered methanogenesis in unsaturated soils (Riley et al., 2011). The ESMs that include CH_4 oxidation in wetlands still represent it as a function of O_2 availability (Wania et al., 2013) despite the widespread occurrence of anaerobic CH_4 oxidation (AOM) in peatlands and other terrestrial ecosystems (Gauthier et al., 2015; Gupta et al., 2013; Smemo & Yavitt, 2007). This emerging understanding of controls on methanogenesis and methanotrophy has thus far been treated as isolated challenges to the classical conceptual model of CH_4 dynamics in peatlands rather than justification to update the conceptual model that underpins the representation of wetland CH_4 dynamics in ESMs.

Here we present an emerging conceptual model that incorporates our improved mechanistic understanding of the pathways and spatial distribution of CH_4 production and oxidation processes (Figure 1). This emerging heterogeneous model acknowledges that methanogenesis is driven by spatial heterogeneity in the relative availability of TEAs versus C (i.e., electron donor) that can lead to the development of methanogenic microsites in partially oxic bulk soil above the water table. Methane produced in drained soil layers can decrease the CH_4 sink strength of the soil if the methanotrophic potential of the soil is constrained by O_2 availability or other factors rather than CH_4 supply. Indeed, a first approximation of microsite CH_4 production in unsaturated soils led to a 20% increase in global CH_4 emissions predicted by CLM4Me, the methane submodel of the Community Land Model (CLM) (Riley et al., 2011). On the other hand, the occurrence of anaerobic CH_4 oxidation (AOM) beneath the water table can attenuate soil CH_4 emissions, potentially oxidizing up to half of the CH_4 produced in northern peatlands (Smemo & Yavitt, 2011). Because these newly described pathways can alter both the direction and magnitude of soil-atmosphere CH_4 fluxes (Figure 1), it is imperative that we assess their inclusion in the conceptual model of peatland CH_4 dynamics. Yet, to date, these pathways have not been considered together in regulating landscape-scale CH_4 fluxes in peatlands.

Evaluation of the classical conceptual model of CH_4 dynamics in peatlands has been limited by the conventional methodologies for quantifying rates of CH_4 production and oxidation. These methods are based on the premise that the conditions for methanogenesis and methanotrophy are mutually exclusive. Gross CH_4 production rates are typically measured in soil slurries incubated in an O_2-free headspace to preclude the possibility of methanotrophy (e.g., Amaral & Knowles, 1994; Mayer & Conrad, 1990). However, the destruction of soil structure in soil slurries alters the availability of C to methanogens to bias estimates of gross rates of methanogenesis (Teh & Silver, 2006). Moreover, the recent discovery of the widespread occurrence of AOM in soils suggests that methanogenesis could be underestimated under anoxic conditions (Blazewicz et al., 2012; Gauthier et al., 2015; Gupta et al., 2013; Smemo & Yavitt, 2007, 2011). Conventional assays for CH_4 oxidation potential, conducted under oxic conditions, can also lead to poor estimates of in situ methanotrophy for multiple reasons: these approaches do not account for AOM (Blazewicz et al., 2012; Smemo & Yavitt, 2007); methanogenesis can occur in reduced microsites in oxic soils (Teh et al., 2005; von Fischer & Hedin, 2007; von Fischer et al., 2009); CH_4 oxidation may be strongly dependent on microsite methanogenesis (Yang & Silver, 2016); and CH_4 dynamics may be non-linearly sensitive to changes in O_2 concentrations (McNicol & Silver, 2015). Moreover, these assays are conducted over widely varying time scales—from hours to days to weeks—with the longer incubations run until CH_4 production or oxidation are stimulated,

therefore likely allowing microbial growth that confounds the interpretation of the measured rates. Importantly, these methods also generally require altering soil structure (e.g., slurrying) or other key characteristics (e.g., soil redox), and thereby do not reflect the in situ distribution of redox conditions, TEAs, and C supply that underpin CH_4 dynamics. In contrast to these common methodologies, the gas phase stable isotope pool dilution technique can be used to simultaneously measure gross CH_4 production and oxidation rates. It has been applied in intact soil core studies in the laboratory (Smemo & Yavitt, 2007) and the field (von Fischer & Hedin, 2002, 2007), mixed soil in the laboratory (Bradley et al., 2012; Gauthier et al., 2015), and also a field study using surface flux chambers for in situ measurements (Yang & Silver, 2016). The stable isotope pool dilution technique is a powerful yet underutilized tool for evaluating CH_4 dynamics in soils where methanogenesis and methanotrophy can co-occur under the full range of redox conditions.

Here we evaluate the classical versus the emerging conceptual model of CH_4 dynamics in peatlands by simultaneously measuring gross rates of CH_4 production and oxidation in a drained temperate peatland using the CH_4 stable isotope pool dilution technique (von Fischer & Hedin, 2002; Yang & Silver, 2016). Flux measurements were conducted both in situ across a microtopographical gradient and ex situ along the soil profile in a temperate peatland that had been drained for agricultural purposes for over a century. Soils collected from above and below the water table were subjected to short-term redox manipulations to investigate patterns in methanogenesis and methanotrophy that could contribute to the landscape-level net CH_4 fluxes. In conjunction with the biogeochemical measurements in the laboratory, we performed quantitative molecular analysis of the microbial community structure to help elucidate drivers of the observed CH_4 dynamics. We expected that the gene abundance of *mcrA*, the key functional gene associated with methanogenesis, would be a good indicator of the genetic potential for methanogenesis to occur given optimal environmental and resource conditions (Angel et al., 2012).

The study site exhibits large CH_4 emissions from drainage ditches, which contribute 84% of the annual ecosystem CH_4 flux despite accounting for a small proportion of the landscape (Teh et al., 2011). According to the classical strata model, we hypothesized that the low CH_4 emissions from the other drier landforms were due to the loss of methanogenesis in the oxic, drained surface soils together with the increased oxidation of CH_4 diffusing upward from the water table through the oxic, unsaturated zone. We, therefore, expected to observe lower gross CH_4 production rates and higher gross CH_4 oxidation rates in the drier landforms compared to the drainage ditch. We also predicted that the highest gross CH_4 production rates would occur from soils collected beneath the water table and the highest gross CH_4 oxidation rates from soils collected just above the water table. In contrast, the emerging heterogeneous conceptual model predicts smaller differences in gross CH_4 production and oxidation rates across the microtopographical gradient and the soil profile because methanogenesis could be maintained in anoxic microsites in the drier landforms and the unsaturated surface soil, and methanotrophy could be maintained by AOM in the drainage ditch and the saturated deep soil. The differences in gross CH_4 production and oxidation rates predicted by the two conceptual models are important to evaluate because we must have the correct conceptual understanding of these component fluxes to accurately predict net CH_4 fluxes under changing environmental conditions.

2. Methods

2.1. Study Site

The study site is a drained peatland pasture located on Sherman Island (38.04°N, 121.75°W) in the Sacramento-San Joaquin River Delta region of Northern California (hereafter, the Delta). The climate is characterized as Mediterranean, with cool, wet winters and hot, dry summers. The mean annual temperature is 15.1°C, and the mean annual precipitation is 335 mm (Hatala et al., 2012). The Delta islands were drained for agricultural purposes around the turn of the twentieth century, leading to high rates of subsidence (Canuel et al., 2009; Deverel et al., 2016; Drexler et al., 2009). The water table is maintained around 50 cm depth by continual pumping (Knox et al., 2015). The soils consist of mucky clay over buried peat and are classified as fine, mixed, superactive, thermic Cumulic Endoaquolls (Drexler et al., 2009). The sapric peat consists of the partially decomposed remains of common reeds (*Phragmites* spp.), cattails (*Typha* spp.), and tules (*Scirpus* spp.) that were deposited in tidal and freshwater marshes that blanketed the Delta region prior to 1800 (Atwater et al., 1979; Whipple et al., 2012), while the current drained pasture vegetation consists of

pepperweed (*Lepidium latifolium*) and the annual mouse barley grass (*Hordeum murinum*) (Sonnentag et al., 2011).

2.2. Methane Dynamics Among Landforms

We divided the study area (0.38 km^2) into four microtopographical landforms that differ primarily in drainage characteristics: crown, slope, hollow/hummock, and drainage ditch (in the sense of Teh et al., 2011). We measured field rates of gross CH_4 production and oxidation in each of the four landforms in October 2007, January 2008, March 2008, and May 2008. We sampled in five replicate plots located 10 m apart along a transect in each landform. Gross CH_4 production and consumption rates were measured using the trace gas pool dilution technique as applied by Yang et al. (2011) to gross N_2O fluxes. Briefly, 15 mL of spiking gas containing 5000 ppm concentration of 3 atom % ^{13}C-CH_4 and 14 ppm concentration of SF_6 in N_2 was injected into the headspace of a two-piece 16 L aluminum chamber inserted 5 cm into the soil surface. This increased the chamber headspace CH_4 concentration by 4.7 ppm and SF_6 concentration by 13 ppb while achieving 2 atom % ^{13}C-CH_4 enrichment. The chamber headspace was sampled at five time points over a 30 min measurement period. We assumed that the fractionation factor associated with CH_4 oxidation was 0.98 (von Fischer & Hedin, 2002). On each sampling date, we measured the ^{13}C-CH_4 enrichment of soil gas sampled from soil equilibration chambers buried at 0–10 cm depth to estimate the ^{13}C composition of the produced soil CH_4; values ranged from 1.0414 to 1.0516 atom % ^{13}C. Gross CH_4 oxidation rates determined from $^{13}CH_4$ tracer loss can be underestimated when gross CH_4 production rates are very high, due to the accumulation of nontrivial amounts of soil-produced ^{13}C-CH_4 in the chamber headspace. Thus, gross CH_4 oxidation rates were calculated from the difference between gross CH_4 production rates and observed net CH_4 fluxes. The methanogenic fraction of C mineralization (F_{MP}) was calculated from gross CH_4 production rates and CO_2 fluxes according to von Fischer and Hedin (2007). We note that gross rates were calculated only for diffusion-driven CH_4 fluxes; ebullition-driven fluxes were identified by the occurrence of a large step change in the chamber headspace concentration of CH_4.

We measured soil temperature and air temperature at the end of each pool dilution measurement. We also collected a soil core (0–10 cm depth) from the chamber footprint to determine gravimetric soil moisture. We calculated volumetric soil moisture and water-filled pore space (WFPS) using soil bulk density values previously measured at the site (Teh et al., 2011).

2.3. Laboratory Soil Depth Profile Experiment

In November 2011, we established a new transect in the hollow/hummock landform with five replicate plots located 10 m apart in preparation for the laboratory experiment to elucidate redox controls on net and gross CH_4 fluxes down the soil profile. This landform was selected for the soil profile experiment because the water table fluctuates below but near the soil surface, allowing us to investigate CH_4 dynamics at the oxic-anoxic interface within the top 1 m of soil. Soil equilibration chambers were installed at 10 cm depth increments to 80 cm depth in each plot for quasi-continuous measurements of soil O_2 and approximately weekly measurements of soil CH_4 concentrations (Text S1 in the supporting information). In March 2012, we performed $^{13}CH_4$ pool dilution measurements in the O_2 transect in the hollow/hummock to determine in situ CH_4 dynamics prior to soil collection for the laboratory soil profile experiment (Text S2 and Table S1). This sampling date was selected based on the 2008 data set showing that the greatest net CH_4 fluxes occurred in March; this also allowed us to obtain a few months of soil gas data from the soil equilibration chambers prior to this experiment. Following the gas measurement, we augered two soil profiles to 80 cm depth from each chamber footprint. We collected the soil in four depth increments based on the current water table position (~35 cm) and O_2 regimes measured by the O_2 sensors during March 2012 (Figure S1): 0–10 (atmospheric), 10–30 (suboxic), 30–60 (oxic-anoxic interface), and 60–80 cm (anoxic). Soils were transported to the laboratory at ambient temperature and were processed the same day.

After gently mixing the soil by hand (i.e., soils were not sieved), we composited the soil from the two profiles collected from within each chamber footprint. We weighed approximately 180 g fresh soil into 1 L Mason jars, with one jar for each of three redox treatments: fresh, oxidized, and reduced. A subsample from each composite sample was air-dried for CN analysis. Replication was at the plot level (n = 5). Perforated plastic wrap was placed over the jars to minimize evaporation while allowing gas exchange during the preincubation period. The fresh treatment samples were preincubated overnight under ambient air to avoid the disturbance

effect from handling the soils while minimizing redox changes; the oxidized treatment samples were preincubated for 3 days under ambient air; and the reduced treatment samples were preincubated for 2 days in an anoxic glove box containing an atmosphere of ultrahigh purity N_2. The oxidized treatment samples were preincubated for a longer period than the reduced treatment samples because we expected that it would take longer for O_2 to diffuse into anoxic microsites likely located within soil aggregates than for O_2 to become depleted in the organic-rich soil. The soils for the reduced treatment remained in the glove box until the last gas sample was taken. All treatments were maintained in the dark and at room temperature (25°C).

For the $^{13}CH_4$ pool dilution measurements, the jars were sealed on viton gaskets using custom-made aluminum lids fitted with Swagelok o-seal fittings containing septa for gas sampling. We injected 10 mL of 4.95 atom % $^{13}CH_4$ at 0.07% concentration and 0.7 ppm SF_6 in N_2 into the jar. Previous work at this study site showed that 30 min was sufficient for the spiking gas to diffuse into the soil as indicated by a stabilization of SF_6 concentrations at 30 min after spiking gas injection. Thus, we sampled 60 mL from each jar at 0.5, 1.5, 2.5, and 3.5 h after spiking gas injection; we stored 30 mL in a preevacuated Wheaton glass vial sealed with an aluminum crimp and a Teflon-coated septum for isotopic analysis and 30 mL in another vial for GC analysis. After sampling we immediately injected either 60 mL of synthetic air (i.e., CH_4 free air) for the ambient air treatments or 60 mL of N_2 for the reduced treatment to maintain the pressure inside of the jars. We corrected for the dilution of the headspace gases caused by replacing the sampled headspace volume. Gross CH_4 production and consumption were determined using the pool dilution model as described for the field measurements. Carbon dioxide emissions were calculated from the linear change in headspace CO_2 concentrations over time.

Immediately before a jar was sealed for $^{13}CH_4$ pool dilution measurements, the soil was gently mixed and subsampled for determination of soil moisture, NH_4^+ and NO_3^- concentrations using 2 *M* KCl extraction, and Fe(II) and Fe(III) concentrations using 0.5 N HCl extraction. Immediately following the last gas sampling, the soil was again mixed and subsampled for microbial DNA analysis. The soil was placed into sterile Whirlpak bags, flash frozen in liquid N_2, and stored in a −80°C freezer.

2.4. Gas and Soil Analysis

Gas samples were analyzed for ^{13}C isotopic composition of CH_4 on a Micromass JA-Series IsoPrime (GV Instruments Ltd, Hudson, NH, USA) continuous flow isotope ratio mass spectrometer interfaced with a TraceGas module located at the Center for Isotope Geochemistry, E.O. Lawrence Berkeley National Laboratory for the field measurements conducted in 2007–2008. The overall precision of the analysis was better than 1%, with a minimum of 0.4 mL of pure CH_4 injected for each analysis. Subsequent isotopic samples were analyzed on an IsoPrime 100 continuous flow isotope ratio mass spectrometer interfaced with a trace gas analyzer (Isoprime Ltd, Cheadle Hulme, UK) at U.C. Berkeley. Both trace gas systems were equipped with a combustion furnace to convert CH_4 to CO_2 for isotopic analysis after CO and CO_2 were scrubbed from the sample. Soil gas samples and duplicate gas samples from pool dilution measurements were analyzed at U.C. Berkeley for CO_2, CH_4, and N_2O concentrations on a Shimadzu GC-14A (Shimadzu Scientific Inc., Columbia, MD, USA) equipped with a thermal conductivity detector, a flame ionization detector, and an electron capture detector. Precision for each detector was $<2\%$.

Soil NH_4^+ and $NO_3^- + NO_2^-$ concentrations in 2 *M* KCl extracts were measured at U.C. Berkeley using a flow injection autoanalyzer (Lachat Instruments, Milwaukee, WI, USA). Soil Fe(III) and Fe(II) concentrations in 0.5 N HCl extracts were measured using a modified ferrozine assay (Liptzin & Silver, 2009). The extracts were analyzed manually on a spectrophotometer at U. C. Berkeley (Genesys 20, Thermo Fisher Scientific, Waltham, MA, USA). Gravimetric soil moisture was determined by drying approximately 10 g soil at 105°C for 48 h.

2.5. Soil Microbial DNA Analysis

Frozen soil samples from the 0–10 cm (surface) and 60–80 cm (deep) depth increments for the fresh and reduced treatments were selected for DNA analysis because these represented the bounds on in situ edaphic and experimental redox conditions experienced by the microbial community. Soil community DNA was extracted from duplicate samples of 0.150 ± 0.001 g oven dry equivalent soil from the 0–10 cm and 60–80 cm depth increments in the fresh and reduced soil treatments. Extractions were performed using

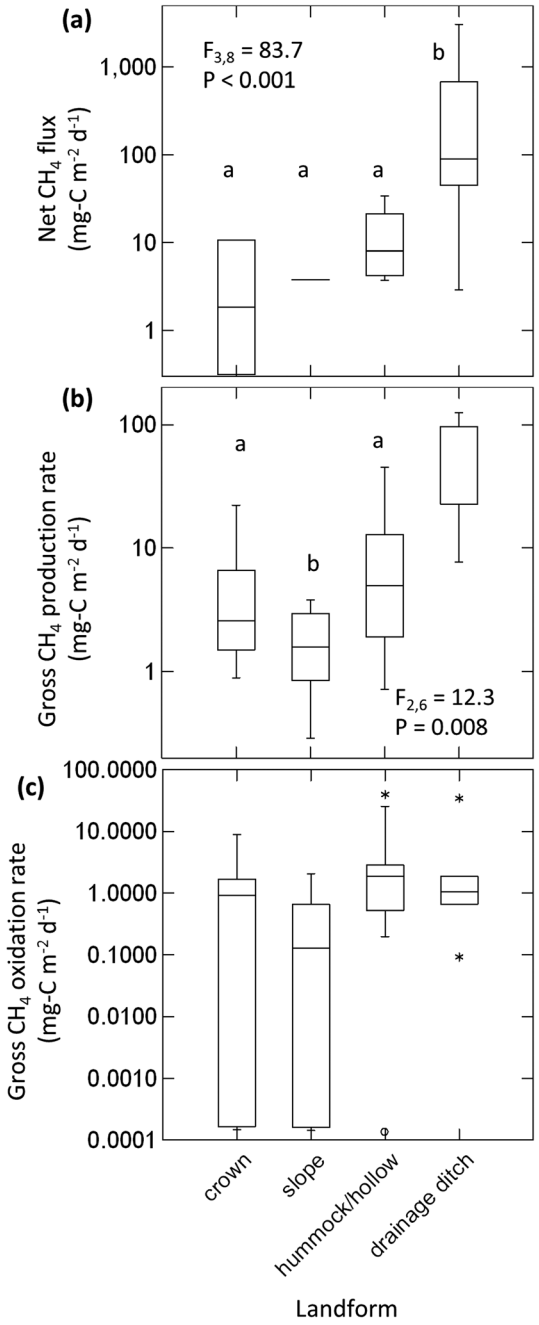

Figure 2. Boxplots of (a) net CH_4 flux, (b) gross CH_4 production rates, and (c) gross CH_4 oxidation rates by landform. *Y* axis is shown on a $\log_{10}$ scale. Letters indicate statistically significant differences among landforms. The drainage ditch was excluded from the statistical analyses comparing gross production and oxidation rates among landforms due to the small number of diffusion driven CH_4 fluxes in this landform.

the Powersoil DNA kit (MoBio Laboratories) with the following modification: in place of the Vortex cell lysis step, beadbeating was completed at 5.5 m s^{-1} for 30 s. Extraction duplicates were combined and further purified using a glycogen/PEG precipitation with ethanol wash and resuspended in 1xTE buffer (Neufeld et al., 2007). DNA was quantified using Quant-iT PicoGreen dsDNA assay (Invitrogen).

Quantitative PCR (qPCR) was conducted on DNA samples to quantify total bacterial 16S (EUB 338/EUB518, Fierer et al., 2005), total archaeal 16S (340f/1000r, Gantner et al., 2011) (340f/1000r Gantner et al., 2011), and total *mcrA* (Banning et al., 2005; Luton et al., 2002). Samples were run in triplicate using a 96-well plate format in a CFX96 thermal cycler equipped with an optical module (BioRad Hercules, CA, USA). All standards were made for qPCR analyses using extracted soil DNA. In brief, qPCR products were cloned into vectors of *Escherichia coli* using a Qiagen PCR Cloning Kit (Qiagen, Valencia, CA, USA) according to manufacturer's instructions. Plasmids were purified using QiaPrep Spin Miniprep Kit (Qiagen, Valencia, CA, USA) and sequenced at the U.C. Berkeley Barker Sequencing Facility and quantified using picogreen.

Each DNA sample was diluted tenfold for qPCR analysis. For total bacterial 16S rRNA gene, total archaeal 16S rRNA gene, and total *mcrA* gene, single reactions were a total of 20 μL: 10 μL Sso Fast Evagreen Supermix (Bio-Rad), 1 μL of forward and reverse primers (10 μM) (Sigma-Aldrich), 7 μL PCR grade MQ-water (MP Biomedicals), and 1 μL of diluted DNA template with an average concentration of 3.55 ng μL^{-1}. The thermocycling parameters for total bacterial 16S were as follows: 3 min at 95°C, followed by 40 cycles of 30 s at 95°C, 30 s at 53°C; and 10 s at 60°C. Fluorescence was measured at the end of each 60°C step. The thermocycling parameters for total bacterial 16S were as follows: 5 min at 95°C, followed by 40 cycles of 10 s at 95°C, 20 s at 57°C, and 5 s at 57°C. Fluorescence was measured at the end of each 57°C step. The thermocycling parameters for total *mcrA* were as follows: 5 min at 95°C, followed by 40 cycles of 10 s at 95°C, 20 s at 50°C, and 5 s at 50°C. Fluorescence was measured at the end of each 50°C step. The PCR efficiency for *mcrA* was 81.6% with a slope of −3.859, and the *mcrA* standard curve had an R^2 value of 0.997. The PCR efficiencies were 96.5% and 82.2% with slopes of −3.409 and −3.839 for bacterial and archaeal 16S, respectively. The standard curves for both bacterial and archaeal 16S had R^2 values >0.98.

2.6. Statistical Analyses

We used SYSTAT version 13 (SPSS Inc., Evanston, IL) to perform statistical analyses and the Microsoft Excel 2013 (Microsoft Corporation, Redmond, WA) to run the iterative pool dilution model. We log-transformed data with nonnormal distributions (all except soil moisture, soil temperature, soil C concentrations, and soil N concentrations) to meet the normality assumptions of analysis of variance (ANOVA) and linear regressions. For the field measurements across the landscape, we performed repeated measures ANOVAs followed by post hoc Fisher's LSD tests with landform as the between-groups factor, sampling date as the within-groups factor, and net and gross CH_4 fluxes as dependent variables. The drainage ditch was excluded for the ANOVA analyses using gross CH_4 production and oxidation rates as the dependent variables because few of the observations in this landform represented diffusive fluxes that can be used in the trace gas stable isotope approach to estimate gross CH_4 fluxes. We used backward stepwise linear regressions to explore the controls on net and gross CH_4 fluxes with possible explanatory variables including WFPS; gravimetric soil moisture; CO_2 emissions (as a proxy for labile C availability); soil

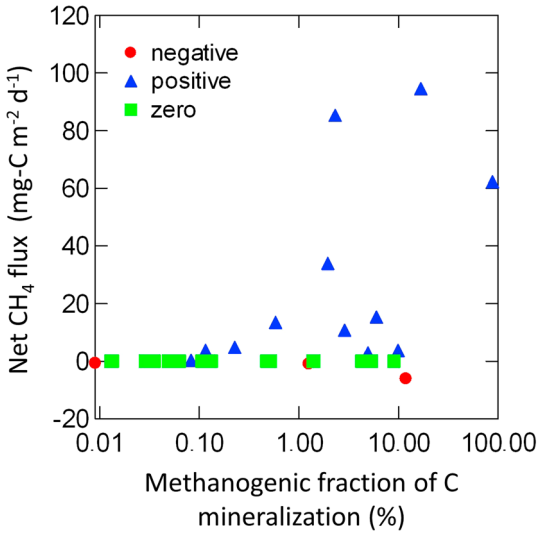

Figure 3. Net CH_4 flux versus methanogenic fraction of C mineralization (F_{MP}). Symbols represent the direction of the net soil-atmosphere CH_4 flux as indicated in the figure legend.

temperature; and gross CH_4 production rates (as a predictor of net CH_4 fluxes and gross CH_4 oxidation rates). We determined the best fit model according to minimal corrected Akaike information criterion (AICc), which reduces the probability of selecting models with extra parameters, using 0.05 as the critical *p* value for retaining explanatory variables in the model. For the laboratory experiment, we performed two-way ANOVAs and post hoc Fisher's LSD multiple comparison tests for a suite of dependent variables, including net and gross CH_4 fluxes as well as soil properties, with the main factors of soil depth, redox treatment, and their interaction. Mean values are reported in the text followed by standard errors (±SEs). Statistical significance was determined at $P < 0.05$ unless otherwise noted.

3. Results

3.1. Environmental Variables Across the Landscape

Across all sampling dates, both gravimetric moisture and WFPS were highest in the drainage ditch and lowest in the crown (Figure S1). Gravimetric soil moisture varied by landform ($F_{3,8} = 37.0$, $P < 0.001$) and by sampling date ($F_{3,24} = 8.43$, $P = 0.001$) with lower soil moisture in May compared to all other sampling dates. Soil moisture differed among landforms in the following order: crown < slope and hummock/hollow < drainage ditch. Water-filled pore space also differed significantly among landform ($F_{3,8} = 115$, $P < 0.001$) and among sampling dates ($F_{3,24} = 10.9$, $P < 0.001$) with a significant interaction between landform and sampling date ($F_{9,24} = 5.00$, $P = 0.001$). Water-filled pore space differed among sampling dates in the following order: May < March and October < January; WFPS was highest in the drainage ditch across all sampling dates, but differences in WFPS among the other landforms differed depending on sampling date.

3.2. Net and Gross CH_4 Fluxes Across the Landscape

Net CH_4 fluxes ranged from −7.4 to 3069 mg C m^{-2} d^{-1} across all landforms and sampling dates. Net CH_4 fluxes averaged 688 ± 276 mg C m^{-2} d^{-1} in the drainage ditch, the lowest lying landform, compared to 0.12 ± 1.08 mg C m^{-2} d^{-1} in the crown, the highest and most well-drained landform (Figure 2a). The fluxes were higher in the drainage ditch than all other landforms ($F_{3,8} = 83.7$, $P < 0.001$) and in March compared to all other sampling dates ($F_{3,24} = 11.8$, $P < 0.001$); there was also a significant interaction between landform and sampling date ($F_{9,24} = 13.0$, $P < 0.001$). Net CH_4 fluxes were positive only when F_{MP} was greater than 0.08%, although negative and zero net CH_4 fluxes occurred across the full range of F_{MP} observed (Figure 3).

Gross CH_4 production associated with diffusive CH_4 fluxes ranged from 0 to 125 mg C m^{-2} d^{-1} across all landforms and sampling dates. Gross CH_4 production and oxidation could only be estimated for diffusion-driven measurements, and in the drainage ditch, 11 out of 16 measurements were identified as being driven by ebullition rather than diffusion. Thus, gross CH_4 production in the drainage ditch, which averaged 69.5 ± 22.9 mg C m^{-2} d^{-1} ($N = 5$), could not be compared against rates in the other landforms. Gross CH_4 production rates were significantly lower in the slope compared to the crown and hummock/hollow ($F_{2,6} = 12.3$, $P = 0.008$; Figure 2b). Average gross CH_4 production rates ranged from 1.3 ± 0.4 mg C m^{-2} d^{-1} in the slope to 3.9 ± 1.9 mg C m^{-2} d^{-1} in the crown and 6.6 ± 3.1 mg C m^{-2} d^{-1} in the hollow/hummock. Gross CH_4 production was positively correlated with F_{MP} ($R^2 = 0.53$, $N = 42$, $P < 0.001$, AICc = 51; Figure 4a) and with WFPS ($R^2 = 0.46$, $N = 44$, $P < 0.001$, AICc = 58; Figure 4b).

Gross rates of CH_4 oxidation ranged from 0 to 39.7 mg C m^{-2} d^{-1} across all landforms and sampling dates. Rates did not differ among landforms or sampling dates (Figure 2c). Overall, gross CH_4 oxidation averaged 3.2 ± 1.2 mg C m^{-2} d^{-1}. Gross CH_4 oxidation rates were not correlated to gross CH_4 production rates or any environmental variable.

3.3. The Soil Depth Profile Experiment

Gravimetric soil moisture increased with depth ($F_{3,16} = 34.3$, $P < 0.001$; Table 1) from 0.39 ± 0.02 g H_2O g^{-1} dry soil at 0–10 cm depth to 0.74 ± 0.01 g H_2O g^{-1} dry soil at 60–80 cm depth. Soil C:N ratios increased with

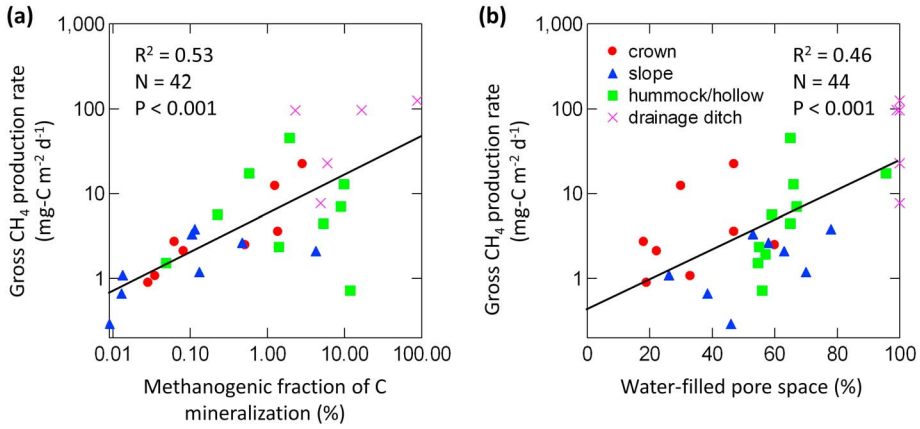

Figure 4. Gross CH_4 production rate versus (a) methanogenic fraction of C mineralization (F_{MP}) and (b) water-filled pore space. Symbols represent different landforms as indicated in the figure legend. The lines represents the linear regression line for all data together.

depth ($F_{3,16}$ = 32.8, $P < 0.001$), ranging from an average of 14.4 ± 0.4 at 0–10 cm depth to an average of 20.7 ± 0.2 at 60–80 cm depth (Table 1). Soil N concentrations ranged from 0.6 to 1.4% and was greatest at 60–80 cm depth ($F_{3,16}$ = 5.50, P = 0.009; Table 1). Soil C concentration ranged from 9.4 to 28.8% and was also greatest at 60–80 cm depth ($F_{3,16}$ = 12.2, $P < 0.001$; Table 1). However, soil CO_2 fluxes (a proxy for labile C availability) in all redox treatments showed a contrasting pattern with depth: 10–30 cm < 30–60 cm < 0–10 cm and 60–80 cm ($F_{3,45}$ = 18.2, $P < 0.001$; Figure 5). Though the same depth pattern held for all redox treatments, overall the fluxes were lowest in the reduced treatment and highest in the fresh treatment ($F_{2,45}$ = 12.7, $P < 0.001$; Figure 5).

Soil concentrations of NH_4^+ generally increased and NO_3^- generally decreased with depth across all redox treatments (NH_4^+: $F_{3,48}$ = 35.6, $P < 0.001$; NO_3^-: $F_{3,48}$ = 12.3, $P < 0.001$; Figures 6a and 6b). The oxidized treatment decreased NH_4^+, and the reduced treatment increased NH_4^+ relative to the fresh treatment (treatment: $F_{2,\ 48}$ = 21.2, $P < 0.001$; Figure 6a). In contrast, the oxidized treatment increased NO_3^-, and the reduced treatment decreased NO_3^- relative to the fresh treatment (treatment: $F_{2,\ 48}$ = 117, $P < 0.001$; Figure 6b). There was a significant interaction between soil depth and redox treatment for soil NO_3^- ($F_{6,48}$ = 6.93, $P > 0.001$), reflecting no differences between fresh and oxidized surface soils (0–30 cm) and no differences among soil depth increments between 10 and 80 cm in the reduced treatment (Figure 6b).

Soil concentrations of 0.5 N HCl-extractable Fe(III) decreased with depth, starting with similarly high concentrations in the two surface soil depth increments ($F_{3,48}$ = 158, $P < 0.001$; Figure 6c). Fe(III) concentrations were significantly lower in the reduced treatment compared to the fresh and oxidized treatments ($F_{2,48}$ = 9.74, $P < 0.001$). Soil concentrations of 0.5 N HCl-extractable Fe(II) differed among soil depths in the following order: 60–80 cm < 0–10 cm and 30–60 cm < 10–30 cm ($F_{3,48}$ = 13.1, $P < 0.001$; Figure 6d). There was a significant interaction between redox treatment and soil depth due to similar Fe(II) concentrations among all soil depths in the oxidized treatment ($F_{6,48}$ = 5.04, $P < 0.001$). Fe(II) concentrations were lowest in the oxidized treatment and highest in the reduced treatment ($F_{2,48}$ = 129, $P < 0.001$).

Table 1
Soil Properties by Soil Depth in the Hummock/Hollow

	Soil depth						
	0–10 cm	10–30 cm	30–60 cm	60–80 cm	df	*F* statistic	*P* value
Soil moisture (g H_2O g^{-1} soil)	0.39 ± 0.02 a	0.43 ± 0.03 a	0.58 ± 0.04 b	0.74 ± 0.01 c	3,16	34.3	< 0.001
C:N ratio	14.4 ± 0.4 a	16.0 ± 0.3 b	17.8 ± 0.8 c	20.7 ± 0.2 d	3,16	32.8	< 0.001
Soil N concentration (%)	0.89 ± 0.06 a	0.73 ± 0.03 a	0.92 ± 0.10 ab	1.15 ± 0.06 b	3,16	12.2	< 0.001
Soil C concentration (%)	12.7 ± 0.5 a	11.7 ± 0.7 a	16.7 ± 2.5 a	23.7 ± 1.3 b	3,16	5.50	0.009

Note: Means ± standard errors (n = 5) are reported. Letters indicate statistically significant differences among soil depths.

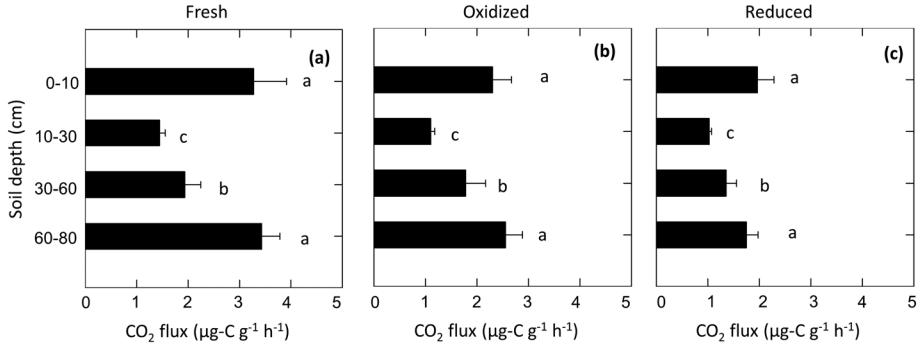

Figure 5. Mean CO_2 fluxes for (a) fresh, (b) oxidized, and (c) reduced soil treatments by soil depth. Error bars represent standard errors. Letters indicate statistically significant differences among soil depths ($F_{3,45} = 18.2$, $P < 0.001$). Soil CO_2 fluxes also differed significantly among all redox treatments ($F_{2,45} = 12.7$, $P < 0.001$).

3.4. Redox Effects on CH_4 Dynamics and Microbial Gene Abundance Along the Soil Depth Profile

Net CH_4 fluxes differed significantly among redox treatments, with negative fluxes (CH_4 uptake) observed in the fresh and oxidized treatments and positive fluxes (emissions) observed in the reduced treatment ($F_{2,44} = 12.5$, $P < 0.001$; Figures 1a–1c). While net CH_4 fluxes were marginally significantly different by soil depth ($F_{3,44} = 2.50$, $P = 0.07$), there was a significant interaction between depth and redox treatment

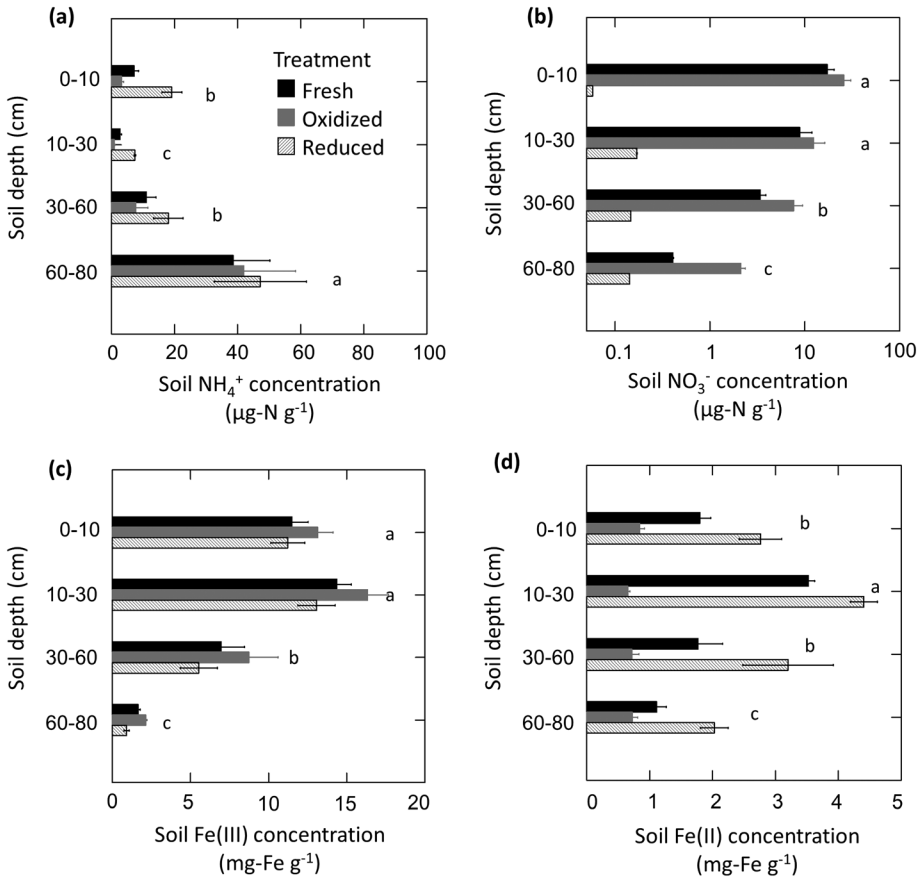

Figure 6. Mean soil (a) NH_4^+ concentrations, (b) NO_3^- concentrations, (c) 0.5 N HCl-extractable Fe(III) concentrations, and (d) Fe(II) concentrations by soil depth and reduced treatment. The *y* axis for Figure 6b is shown on a $\log_{10}$ scale. Error bars represent standard errors. Letters indicate statistically significant differences ($P < 0.05$) among soil depths across all redox treatments, except for soil NO_3^- in the reduced treatment and Fe(II) in the oxidized treatment where there were significant interactions of soil depth and redox treatment.

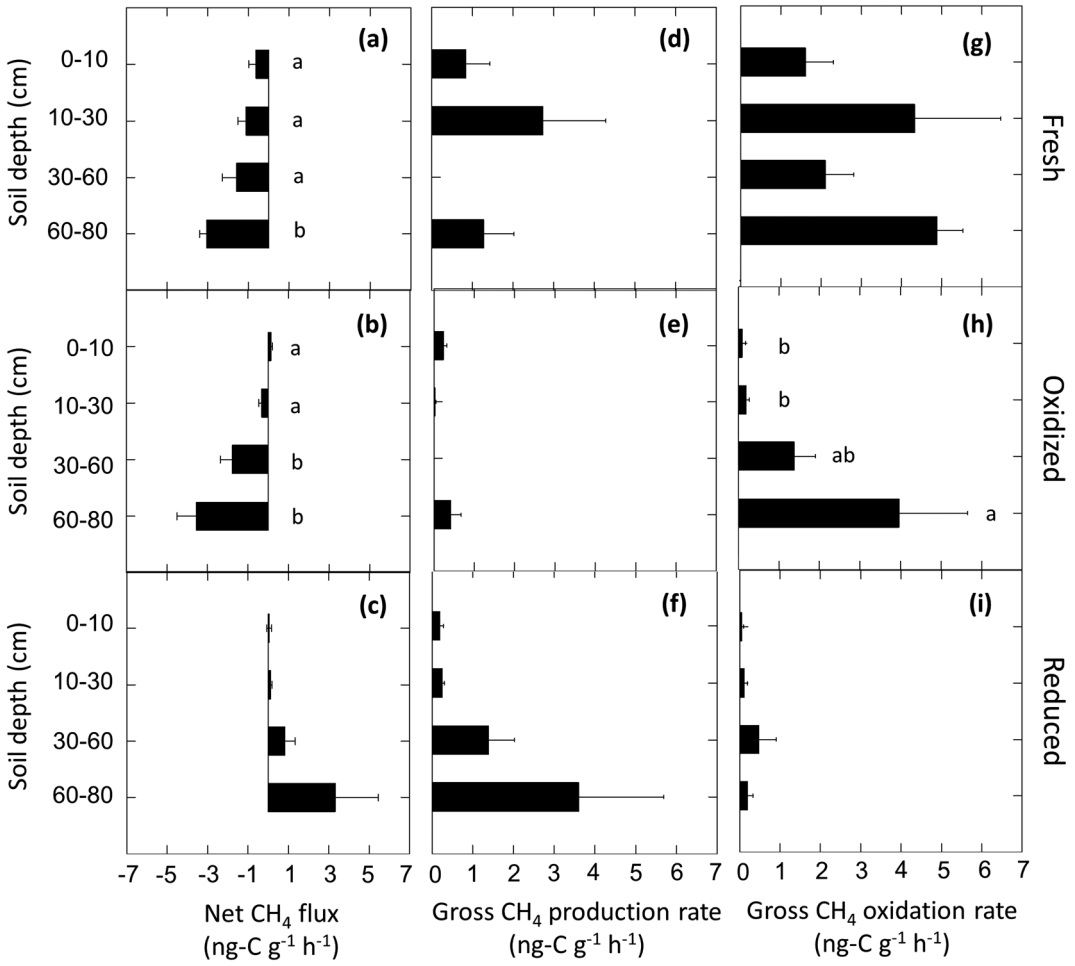

Figure 7. (a–c) Mean net CH_4 fluxes, (d–f) mean gross CH_4 production rates, and (g–i) mean gross CH_4 oxidation rates by soil depth and headspace treatment (shown in different panels). Error bars represent standard errors. Letters indicate statistically significant differences among soil depths at $P < 0.05$ determined using Fisher's LSD following a two-way ANOVA with soil depth and redox treatment as factors.

($F_{6,44} = 4.38$, $P = 0.002$). This reflects significantly higher CH_4 uptake rates in deep soils compared to surface soils in the fresh and oxidized treatments ($P < 0.05$; Figures 7a and 7b); in contrast, CH_4 emissions trended higher with soil depth in the reduced treatment, but this was not a statistically significant effect (Figure 7c).

Gross CH_4 production rates were marginally significantly different among redox treatments, with lower rates in the oxidized treatment compared to the fresh and reduced treatments ($F_{2,42} = 2.63$, $P = 0.08$; Figures 7d–7f). Gross CH_4 production rates decreased with soil depth in the reduced treatment ($P < 0.01$; Figure 7f), whereas there were no depth trends in the other redox treatments (Figures 7d and 7e). However, the interaction between depth and redox treatment was significant only at $P = 0.10$ ($F_{6,42} = 1.89$). Gross CH_4 production rates were strongly positively correlated to F_{MP} across all soil depths and headspace treatments ($R^2 = 0.87$, $N = 54$, $P < 0.001$, Figure 8).

Gross CH_4 oxidation rates were highest in the fresh treatment and lowest in the reduced treatment ($F_{2,42} = 11.8$, $P < 0.001$; Figures 7g–7i). Gross CH_4 oxidation rates were significantly higher in the deepest soil increment (60–80 cm) compared to all other soil depths ($F_{3,42} = 4.20$, $P = 0.01$). Although no significant interaction between soil depth and redox treatment was detected ($F_{6,42} = 1.60$, $P = 0.17$), there was a trend toward increasing gross CH_4 oxidation that emerged in the oxidized treatment only (Figure 7h).

Gene copy numbers of bacterial 16S rRNA, archaeal 16S rRNA, and *mcrA* did not differ significantly between surface (0–10 cm) and deep (60–80 cm) soils nor between the fresh and reduced treatments (Figure 9).

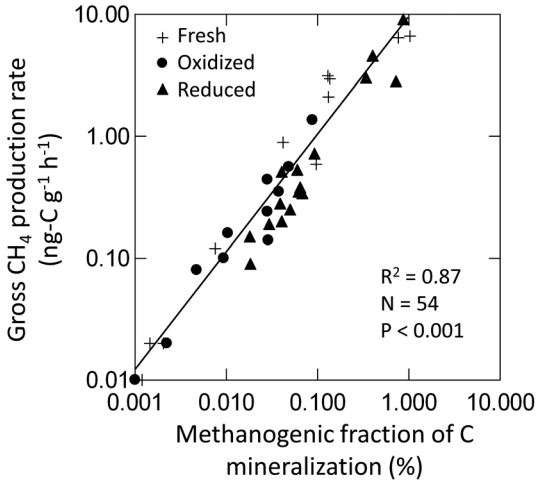

Figure 8. Gross CH_4 production rate versus methanogenic fraction of C mineralization (F_{MP}). Symbols represent different soil depths as indicated in the figure legend. The line represents the linear regression line for all data.

4. Discussion

4.1. Microtopographical Variation in CH_4 Dynamics

Field measurements of net and gross CH_4 fluxes lended support to the emerging heterogeneous conceptual model, which predicted less variation in gross CH_4 production and oxidation across the microtopographical gradient than the classical strata conceptual model. Net CH_4 fluxes were greatest in the drainage ditches across all four sampling dates, consistent with landscape patterns in annual surface flux estimates reported by Teh et al. (2011) for this site. Rather than being driven by both higher gross CH_4 production and lower gross CH_4 oxidation in the drainage ditches, which were at or near-saturation in surface soils on all sampling dates, this pattern in net CH_4 fluxes was driven entirely by variation in methanogenesis. Gross CH_4 oxidation rates were similar among all landforms despite a wide range in WFPS in surface soils. von Fischer and Hedin (2002) similarly found a wider range in gross CH_4 production rates (0.04–930 mg C m^{-2} d^{-1}) than in gross CH_4 oxidation rates (0.1–9.2 mg C m^{-2} d^{-1}) for soil cores collected from temperate and tropical ecosystems. They hypothesized that gross CH_4 oxidation rates are more constrained than gross CH_4 production rates because methanotrophy depends on the availability of both CH_4 and O_2, and conditions that increase their availability are mutually exclusive. While this may be true in soil cores, according to the classical strata model of CH_4 dynamics, we expected that the spatial segregation between dominant sites of methanogenesis and methanotrophy along the soil profile would lead to the greatest CH_4 oxidation rates in the higher landforms where CH_4 produced at depth would travel through more O_2-rich soil with high potential for methanotrophy before reaching the atmosphere. The emerging conceptual model would invoke AOM to explain how gross rates of CH_4 oxidation in the drainage ditches could have been comparable to those in the drier landforms, which may have exhibited only O_2-dependent methanotrophy above the water table. Alternatively, if AOM did not occur anywhere in the peatland, then O_2-dependent methanotrophy may have been limited by O_2 availability in the drainage ditches and by CH_4 availability in the drier landforms to yield similar gross CH_4 oxidation rates across the peatland. While roots can act as conduits for rhizosphere oxygenation to support CH_4 oxidation in bulk anoxic soil (Bellisario et al., 1999; Frenzel et al., 1992; Popp et al., 2000), the drainage ditches at our site were unvegetated. In addition, the vegetated drier landforms lacked vascular plants that can decrease soil CH_4 oxidation rates by transporting CH_4 from the soil to the atmosphere through aerenchyma (Butterbach-Bahl et al., 1997; Knoblauch et al., 2015; Shannon et al., 1996). In sections 4.2 and 4.3, we discuss the complex controls on CH_4 dynamics throughout the soil profile in order to better understand and interpret these landscape-scale patterns in CH_4 production and oxidation.

Our results are consistent with other studies suggesting that variation in methanogenesis is more important than methanotrophy in controlling net CH_4 fluxes (Goodrich et al., 2015; von Fischer & Hedin, 2007). Across the landscape, net CH_4 emissions occurred only above a threshold value of 0.08% for F_{MP}, a measure of C flow

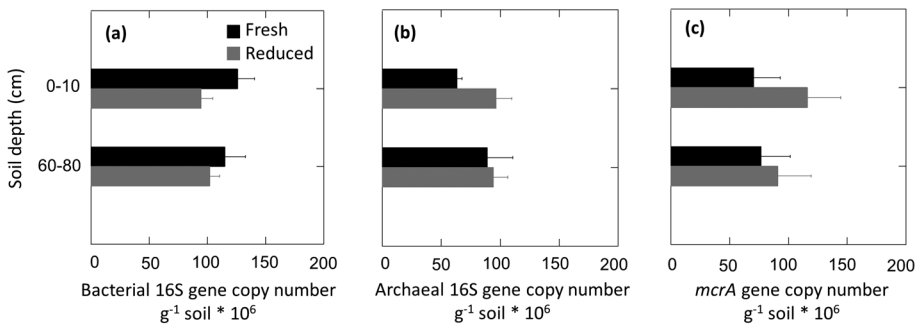

Figure 9. Gene copy numbers of (a) bacterial 16S rRNA, (b) archaeal 16S rRNA, and (c) *mcrA*, the key functional gene associated with methanogenesis, determined using qPCR of DNA extracted from soil samples in the laboratory soil depth profile experiment. Error bars represent standard errors.

through methanogenic pathways that was positively correlated to gross CH_4 production rates. This finding suggests that the proportion of C flow through methanogenic pathways is one of the dominant controls on CH_4 efflux, rather than the rate of CH_4 oxidation or the C mineralization rate (von Fischer & Hedin, 2007). Our F_{MP} threshold value was comparable to the 0.04% F_{MP} threshold determined by von Fischer and Hedin (2007) for a variety of upland temperate and tropical soils. In contrast, in a nearby Delta cornfield, no net CH_4 fluxes were detectable despite F_{MP} reaching as high as 0.27% (Yang & Silver, 2016). Disturbance to soil structure associated with planting and tillage in the cornfield may have created more macropores for O_2 to diffuse into the soil to sustain CH_4 oxidation that could keep pace with CH_4 production, leading to no net soil-atmosphere CH_4 efflux despite exhibiting a higher F_{MP} value than that observed by von Fischer and Hedin (2007). This suggests that the F_{MP} threshold above which net CH_4 emissions occur is an emergent property based on factors controlling O_2 availability to methanotrophs in the bulk soil and redox conditions for methanogens in soil microsites, such as located within soil aggregates (Sexstone et al., 1985) or near labile C sources that fuel high heterotrophic activity (Parkin, 1987).

4.2. Controls on Methanogenesis Along the Soil Profile

In support of the emerging heterogeneous model of CH_4 dynamics, we found that the abundance of highly reducing microsites (estimated as F_{MP}) was a more important control on gross CH_4 production rates than the saturation or O_2 status of the bulk soil. We observed similar gross rates of CH_4 production in fresh soils collected from above and below the water table. To demonstrate that CH_4 production in the unsaturated soils was occurring in highly reducing microsites, we incubated the soils in the laboratory under ambient air, causing concomitant oxidation of the soil Fe(II) pools and inhibition of methanogenesis. The similar gene abundance of *mcrA*, the key functional gene associated with methanogenesis, in the permanently drained surface soil and the permanently flooded deep soil suggest comparable genetic potential for methanogenesis to occur across the soil profile when highly reducing conditions develop in soil microsites or the bulk soil.

Notably, F_{MP}, which is an index of the abundance of highly reducing soil microsites, explained nearly all (87%) of the variability in gross CH_4 production rates across all soil depths and laboratory redox treatments. The explanatory power of the F_{MP} likely stemmed from the wide range in observed values across two orders of magnitude from less than 0.01% to approximately 1%, indicating intense and dynamic changes in competition between methanogenesis and other respiratory pathways within and among soil depths and redox treatments. This wide range for F_{MP} is not predicted by the coarse changes in bulk soil O_2 observed in situ along these depth increments, or by the redox end-member treatments imposed during the laboratory incubations, which would predict similar step changes in CH_4 dynamics. These results are instead consistent with the findings of other recent studies whereby bulk soil O_2 measurements have been shown to effectively characterize long-term and average soil environmental conditions but may not accurately capture the short-term or fine-scale dynamics of soil O_2 and redox-sensitive processes such as methanogenesis, particularly when there is an abundance of competing TEA processes (Askaer et al., 2010; Knorr & Blodau, 2009; Silver et al., 2013). The Delta setting and land use history at our study site has led to an abundance of soil Fe and mineral N that may have driven the observed competition between methanogenesis and other respiratory pathways, increased the variability and sensitivity of F_{MP}, and caused bulk soil oxygen or C to be poor predictors of CH_4 flux.

Patterns in gross CH_4 production in the reduced treatment revealed how spatial heterogeneity in resources could exert complex controls on methanogenesis. Gross CH_4 production rates in surface soils trended toward lower values in the reduced compared to the fresh redox treatment, which demonstrated substantial spatial heterogeneity in soil redox conditions based on high concentrations of both NO_3^- and Fe(II) (presumably present in the oxic bulk soil and in anoxic soil microsites, respectively). Incubation under an N_2 headspace created more homogenous and lower redox conditions throughout the soil as evidenced by an increase in Fe(II) to even higher concentrations accompanied by a decrease in NO_3^- to near undetectable levels. Despite the absence of O_2 and more reduced soil conditions, methanogenesis was likely suppressed in the surface soils by mechanisms relating to substrate specificity and limitation. Dissimilatory Fe reducers can outcompete methanogens for key C substrates (Lovley & Phillips, 1987; Roden & Wetzel, 2003; Teh et al., 2008), primarily due to a greater affinity for acetate (Roden & Wetzel,

2003). Our results suggest that the greater competitiveness of the Fe reducers was likely also a function of the spatial extent of Fe reduction through the anoxic bulk soil fueled by the large surface soil pools of HCl-extractable Fe(III), which are considered readily reducible by microbes (Lovley & Phillips, 1986a, 1986b). In the fresh treatment, the demand for acetate by aceticlastic methanogens likely caused diffusion of acetate toward highly reducing microsites, but in the reduced treatment, the stronger demand for acetate by Fe reducers throughout the bulk soil may have suppressed this diffusion of acetate toward methanogenic microsites. In this way, methanogenesis can be sustained in unsaturated soils with spatially heterogeneous redox conditions and suppressed in soils with homogenous lower redox conditions induced by flooding or anoxic headspace incubation.

The suppression of methanogenesis in the reduced treatment was not observed for the deep soils from the organic peat horizons despite comparably high Fe reduction rates under anoxic conditions in the surface and deep soils (as deduced from differences in Fe(II) concentrations between the fresh and reduced treatments). We postulate that this is due to the domination of fermentative rather than dissimilatory Fe reduction (Lovley, 1987; Reiche et al., 2008), thereby linking acetate production rather than consumption to Fe reduction. Alternatively, methanogenesis may have been dominated by hydrogenotrophic rather than aceticlastic pathways in the deep soils. Across all redox treatments, soil CO_2 fluxes were similarly high at 0–10 cm and 60–80 cm depth despite a nearly twofold increase in total SOC from the surface to depth. Labile C inputs from roots above the water table could have driven high C mineralization rates in the surface soil, whereas high CO_2 fluxes in the deep soil may have been sustained by a larger but more recalcitrant total SOC pool. While this difference in methanogenic pathway associated with a decrease in C lability from the soil surface to depth could rule out competitive inhibition of aceticlastic methanogenesis by dissimilatory Fe reducers (Hodgkins et al., 2015; Hornibrook, 1997), hydrogenotrophic methanogenesis can also be directly inhibited by Fe(III) because some hydrogenotrophic methanogens can reduce Fe(III) by using H_2 as the electron donor (Bond & Lovley, 2002; Reiche et al., 2008; van Bodegom et al., 2004). Although the role of Fe reduction in inhibiting methanogenesis has been demonstrated in many different ecosystems (e.g., Frenzel et al., 1999; Miller et al., 2015; Roden & Wetzel, 2003; Teh et al., 2008), our results suggest that this mechanism may not universally apply—even within a study site—and that characterization of the microbial community could elucidate when it is important (Graham et al., 2016).

4.3. Controls on Methanotrophy Along the Soil Profile

Our data suggest that AOM was not an important process in soils from the drained landforms in the peatland. In the laboratory experiment using soils from the hummock/hollow landform, gross CH_4 oxidation rates were suppressed to near zero for all soil depths in the reduced treatment, indicating that CH_4 oxidation was inhibited by the absence of O_2. Anaerobic CH_4 oxidation has been observed in many peatland soils incubated under high (percent level) CH_4 concentrations (Blazewicz et al., 2012; Gupta et al., 2013; Smemo & Yavitt, 2007). Thus, AOM may require CH_4 concentrations higher than those used in our incubation (10 ppm) and observed in the hummock/hollow (maximum of 1784 ppm). Gauthier et al. (2015) reported widespread AOM in soils using 20 ppm $^{13}CH_4$ incubations, but the rates were low (averaging 0.25 ng C g^{-1} h^{-1}); we measured comparably low gross CH_4 oxidation rates on some individual soil samples in the reduced treatment, but the soil depth means were not significantly different from zero. Higher gross CH_4 production rates and slower gas transport through the saturated surface soils of the drainage ditches may have led to high enough soil CH_4 concentrations to support AOM in that landform.

The laboratory experiment unexpectedly illuminated a novel control on O_2-dependent methanotrophy that extends beyond substrate limitation by O_2 and CH_4. Gross CH_4 oxidation was tightly coupled to gross CH_4 production in the hummock/hollow surface soils (0–30 cm depth) such that net CH_4 fluxes were small or near zero regardless of soil redox status. In the oxidized treatment, methanotrophy was not stimulated by increased soil O_2 availability as expected but, rather, was suppressed along with methanogenesis. This strong dependence of methanotrophy on methanogenesis was also observed in in situ field measurements of gross CH_4 fluxes in a nearby cornfield on a similar soil type (Yang & Silver, 2016) but with a lower water table depth of 80–120 cm (Knox et al., 2015). Yang and Silver (2016) hypothesized that rather than simply reflecting the limitation of methanotrophy by CH_4 availability, this dependence of methanotrophy on methanogenesis could be due to a combination of mechanisms localizing methanotrophy in or near highly active methanogenic microsites where CH_4 concentrations may be high. Activity by low affinity Type I methanotrophs, who

consume CH_4 only at high concentrations (Bender & Conrad, 1992, 1995), or a shift in the CH_4 monooxygenase (MMO) enzyme affinity of Type II methanotrophs from high to low (Dunfield et al., 1999) would lead to MMO enzymes in the bulk soils incapable of oxidizing CH_4 at the relatively low incubation headspace concentrations of 10 ppm. Furthermore, it is possible that only methanotrophs exposed to high CH_4 concentrations in or near methanogenic microsites could synthesize MMO enzymes given that nearly all observations of in situ soil CH_4 concentrations at 0–30 cm depths were below 100 ppm, which is not high enough to induce methanotrophic activity in the bulk soil (Bender & Conrad, 1995; Cai et al., 2016; Nesbit & Breitenbeck, 1992). The overall effect of these mechanisms is that methanotrophs in the surface soil would have little capacity to oxidize CH_4 beyond what was produced in methanogenic microsites and thus could not contribute to the attenuation of CH_4 emissions as predicted by the classical conceptual model of peatland CH_4 dynamics.

In contrast to the surface soils, the deep soils (30–80 cm depth) from the hummock/hollow acted as strong CH_4 sinks when O_2 was available in the fresh and oxidized treatments, as predicted by the classical conceptual model. In the deep soils, gross CH_4 oxidation rates were unaffected by the inhibition of methanogenesis in the oxidized treatment, suggesting that methanotrophs were able to consume exogenous CH_4 away from methanogenic microsites. In situ soil CH_4 concentrations at 30–80 cm depth were high enough (ranging from 100 to 10,000 ppm) to induce methanotrophic activity in the bulk soil such that CH_4 oxidation was not limited to methanogenic microsites as it was in the surface soils (Bender & Conrad, 1992; Cai et al., 2016; Nesbit & Breitenbeck, 1992). This induction by high bulk soil CH_4 concentrations can enable soils from the oxic-anoxic interface at the water table to act as strong CH_4 sinks when the water table is lowered (Happell & Chanton, 1993; Kettunen et al., 1999; van den Pol-Van Dasselaar et al., 1999). This induction effect lasts on the order of weeks to months (Cai et al., 2016; Yavitt, 2013). Therefore, short-term fluctuations in water table depth can lead to recently drained soil layers attenuating CH_4 produced from lower in the soil profile as predicted by the classical conceptual model. However, as observed in the permanently unsaturated soils of our drained peatland, with longer term drainage, the unsaturated surface soils could lose this function and only serve to attenuate endogenous CH_4 produced within highly reduced microsites in the oxic bulk soil.

5. Conclusions

Our data support the need to update the classical strata conceptual model of peatland CH_4 dynamics with our emerging understanding of controls on the heterogeneous distribution of methanogenesis and methanotrophy above and below the water table. Although the patterns in net CH_4 fluxes were consistent with the classical model, with higher effluxes in the flooded or saturated drainage ditches compared to the portions of the landscape with a deeper water table, the patterns in gross CH_4 production and oxidation across the microtopographical gradient and along the soil profile could not be explained by water table position. Rather than the loss of methanogenesis coupled with an increase in methanotrophy in the oxic, unsaturated surface layers leading to lower net CH_4 effluxes in the higher landforms compared to the drainage ditches, we observed CH_4 dynamics that were even more complex than we had hypothesized.

Our soil profile data supported the emerging heterogeneous conceptual model that includes methanogenesis occurring within highly reducing microsites in oxic soil above the water table. However, the oxic, unsaturated soil did not act as a sink for atmospheric CH_4 because gross rates of CH_4 production and oxidation were unexpectedly tightly coupled. In contrast, the sapric peat collected from beneath the water table switched between acting as strong net CH_4 source and sink based on redox conditions. This redox response of the deeper sapric peat CH_4 dynamics was more consistent with observations from undrained peatlands experiencing a temporary lowering of the water table (Goodrich et al., 2015; Roulet et al., 1993; Updegraff et al., 2001). This suggests a difference in the potential for methanotrophy to attenuate soil CH_4 emissions under short-term fluctuations in water table depth versus long-term drainage (whether intentionally or as a result of climate change), the latter of which leads to lower organic C content such as in the surface soils in our site. Our data also suggest that AOM may not universally occur in anoxic peatland soils but is mediated by high CH_4 concentrations. We did not observe AOM in the hummock/hollow soils where in situ soil CH_4 concentrations were low; however, the drainage ditch, which was dominated by ebullition-driven CH_4 fluxes suggesting high soil CH_4 concentrations, may have been able to support similar gross CH_4 oxidation rates to

the other landforms through AOM. The simultaneous measurements of gross CH_4 production and oxidation both in situ and ex situ gave us novel insight into the component fluxes leading to the observed landscape-level net CH_4 fluxes, including unexpected responses of methanogenesis and methanotrophy to redox manipulations that warrant further investigation to determine their importance in other drained peatlands and other peatland types. We conclude that our ability to predict peatland CH_4 fluxes will improve by refining the emerging conceptual model and moving beyond the constraints of the classical strata conceptual model of peatland CH_4 dynamics that focuses on water table position as the dominant driver of methanogenesis and methanotrophy.

Acknowledgments
We appreciate discussions with M. Firestone and S. Blazewicz. We received assistance in the field and lab from K. Smetak, H. Dang, and A. McDowell. This research was funded by grants to W.L.S. from the U.S. National Science Foundation (ATM-0842385 and DEB-0543558) and the California Department of Fish and Wildlife (CDFW) and California Department of Water Resources (DWR) contract 4600011240. The data used are listed in the references, tables, supporting information, and the Illinois Digital Environment for Access to Learning and Scholarship (IDEALS) repository at https://www.ideals.illinois.edu/.

References

Adamsen, A. P., & King, G. M. (1993). Methane consumption in temperate and subarctic forest soils: Rates, vertical zonation, and responses to water and nitrogen. *Applied and Environmental Microbiology*, *59*, 485–490.

Alm, J., Schulman, L., Walden, J., Nykanen, H., Martikainen, P. J., & Silvola, J. (1999). Carbon balance of a boreal bog during a year with an exceptionally dry summer. *Ecology*, *80*(1), 161–174. https://doi.org/10.2307/176987

Amaral, J. A., & Knowles, R. (1994). Methane metabolism in a temperate swamp. *Applied and Environmental Microbiology*, *60*(11), 3945–3951.

Angel, R., Claus, P., & Conrad, R. (2012). Methanogenic archaea are globally ubiquitous in aerated soils and become active under wet anoxic conditions. *The ISME Journal*, *6*(4), 847–862. https://doi.org/10.1038/ismej.2011.141

Askaer, L., Elberling, B., Glud, R. N., Kuhl, M., Lauritsen, F. R., & Joensen, H. R. (2010). Soil heterogeneity effects on O_2 distribution and CH_4 emissions from wetlands: In situ and mesocosm studies with planar O_2 optodes and membrane inlet mass spectrometry. *Soil Biology and Biochemistry*, *42*(12), 2254–2265. https://doi.org/10.1016/j.soilbio.2010.08.026

Atwater, B. F., Conard, S. G., Dowden, J. N., Hedel, C. W., MacDonald, R. L., & Savage, W. (1979). History, landforms, and vegetation of the estuary's tidal marshes. In T. J. Conomos, A. E. Leviton, & M. Berson (Eds.), *San Francisco Bay: The Urbanized Estuary* (pp. 347–396). San Francisco, CA: Pacific Division of the American Association for the Advancement of Science.

Banning, N., Brock, F., Fry, J. C., Parkes, R. J., Hornibrook, E. R. C., & Weightman, A. J. (2005). Investigation of the methanogen population structure and activity in a brackish lake sediment. *Environmental Microbiology*, *7*(7), 947–960. https://doi.org/10.1111/j.1462-2920.2004.00766.x

Beal, E. J., House, C. H., & Orphan, V. J. (2009). Manganese- and iron-dependent marine methane oxidation. *Science*, *325*(5937), 184–187. https://doi.org/10.1126/science.1169984

Bellisario, L. M., Bubier, J. L., Moore, T. R., & Chanton, J. P. (1999). Controls on CH_4 emissions from a northern peatland. *Global Biogeochemical Cycles*, *13*, 81–91. https://doi.org/10.1029/1998GB900021

Bender, M., & Conrad, R. (1992). Kinetics of CH_4 oxidation in oxic soils exposed to ambient air or high CH_4 mixing ratios. *FEMS Microbiology Ecology*, *101*(4), 261–270. https://doi.org/10.1111/j.1574-6968.1992.tb05783.x

Bender, M., & Conrad, R. (1994). Methane oxidation activity in various soils and freshwater sediments: Occurrence, characteristics, vertical profiles, and distribution on grain size fractions. *Journal of Geophysical Research: Atmospheres*, *99*, 16,531–16,540. https://doi.org/10.1029/94JD00266

Bender, M., & Conrad, R. (1995). Effect of CH_4 concentrations and soil conditions on the induction of CH_4 oxidation activity. *Soil Biology and Biochemistry*, *27*(12), 1517–1527. https://doi.org/10.1016/0038-0717(95)00104-M

Blazewicz, S. J., Petersen, D. G., Waldrop, M. P., & Firestone, M. K. (2012). Anaerobic oxidation of methane in tropical and boreal soils: Ecological significance in terrestrial methane cycling. *Journal of Geophysical Research: Biogeosciences*, *117*, G02033. https://doi.org/10.1029/2011JG001864

Bond, D. R., & Lovley, D. R. (2002). Reduction of Fe(III) oxide by methanogens in the presence and absence of extracellular quinones. *Environmental Microbiology*, *4*(2), 115–124. https://doi.org/10.1046/j.1462-2920.2002.00279.x

Bradley, R. L., Chronakova, A., Elhottova, D., & Simek, M. (2012). Interactions between land-use history and earthworms control gross rates of soil methane production in an overwintering pasture. *Soil Biology and Biochemistry*, *53*, 64–71. https://doi.org/10.1016/j.soilbio.2012.04.025

Butterbach-Bahl, K., Papen, H., & Rennenberg, H. (1997). Impact of gas transport through rice cultivars on methane emission from rice paddy fields. *Plant, Cell & Environment*, *20*(9), 1175–1183. https://doi.org/10.1046/j.1365-3040.1997.d01-142.x

Cai, Y. F., Zheng, Y., Bodelier, P. L. E., Conrad, R., & Jia, Z. J. (2016). Conventional methanotrophs are responsible for atmospheric methane oxidation in paddy soils. *Nature Communications*, *7*, 10. https://doi.org/10.1038/ncomms11728

Canuel, E. A., Lerberg, E. J., Dickhut, R. M., Kuehl, S. A., Bianchi, T. S., & Wakeham, S. G. (2009). Changes in sediment and organic carbon accumulation in a highly-disturbed ecosystem: The Sacramento-San Joaquin River Delta (California, USA). *Marine Pollution Bulletin*, *59*(4–7), 154–163. https://doi.org/10.1016/j.marpolbul.2009.03.025

Ciais, P., Sabine, C., Bala, G., Bopp, L., Brovkin, V., Canadell, J., … Thornton, P. (2013). Carbon and other biogeochemical cycles. In T. F. Stocker, et al. (Eds.), *Climate Change 2013: The Physical Science Basis. Contribution of Working Group I to the Fifth Assessment Report of the Intergovernmental Panel on Climate Change* (pp. 465–570). Cambridge, United Kingdom and New York, NY: Cambridge Univ. Press.

Deverel, S. J., Ingrum, T., & Leighton, D. (2016). Present-day oxidative subsidence of organic soils and mitigation in the Sacramento-San Joaquin Delta, California, USA. *Hydrogeology Journal*, *24*(3), 569–586. https://doi.org/10.1007/s10040-016-1391-1

Drexler, J. Z., de Fontaine, C. S., & Deverel, S. J. (2009). The legacy of wetland drainage on the remaining peat in the Sacramento-San Joaquin Delta, California, USA. *Wetlands*, *29*(1), 372–386. https://doi.org/10.1672/08-97.1

Dunfield, P. F., Liesack, W., Henckel, T., Knowles, R., & Conrad, R. (1999). High-affinity methane oxidation by a soil enrichment culture containing a type II methanotroph. *Applied and Environmental Microbiology*, *65*(3), 1009–1014.

Fenner, N., & Freeman, C. (2011). Drought-induced carbon loss in peatlands. *Nature Geoscience*, *4*(12), 895–900. https://doi.org/10.1038/ngeo1323

Fetzer, S., Bak, F., & Conrad, R. (1993). Sensitivity of methanogenic bacteria from paddy soil to oxygen and desiccation. *FEMS Microbiology Ecology*, *12*, 107–115. https://doi.org/10.1111/j.1574-6941.1993.tb00022.x

Fierer, N., Jackson, J. A., Vilgalys, R., & Jackson, R. B. (2005). Assessment of soil microbial community structure by use of taxon-specific quantitative PCR assays. *Applied and Environmental Microbiology*, *71*(7), 4117–4120. https://doi.org/10.1128/AEM.71.7.4117-4120.2005

Frenzel, P., Bosse, U., & Janssen, P. H. (1999). Rice roots and methanogenesis in a paddy soil: Ferric iron as an alternative electron acceptor in the rooted soil. *Soil Biology and Biochemistry*, *31*(3), 421–430. https://doi.org/10.1016/S0038-0717(98)00144-8

Frenzel, P., Rothfuss, F., & Conrad, R. (1992). Oxygen profiles and methane turnover in a flooded rice microcosm. *Biology and Fertility of Soils*, *14*(2), 84–89. https://doi.org/10.1007/BF00336255

Gantner, S., Andersson, A. F., Alonso-Saez, L., & Bertilsson, S. (2011). Novel primers for 16S rRNA-based archaeal community analyses in environmental samples. *Journal of Microbiological Methods*, *84*(1), 12–18. https://doi.org/10.1016/j.mimet.2010.10.001

Gauthier, M., Bradley, R. L., & Simek, M. (2015). More evidence that anaerobic oxidation of methane is prevalent in soils: Is it time to upgrade our biogeochemical models? *Soil Biology and Biochemistry*, *80*, 167–174. https://doi.org/10.1016/j.soilbio.2014.10.009

Goodrich, J. P., Campbell, D. I., Roulet, N. T., Clearwater, M. J., & Schipper, L. A. (2015). Overriding control of methane flux temporal variability by water table dynamics in a Southern Hemisphere, raised bog. *Journal of Geophysical Research: Biogeosciences*, *120*, 819–831. https://doi.org/10.1002/2014JG002844

Graham, E. B., Knelman, J. E., Schindlbacher, A., Siciliano, S., Breulmann, M., Yannarell, A., … Nemergut, D. R. (2016). Microbes as engines of ecosystem function: When does community structure enhance predictions of ecosystem processes? *Frontiers in Microbiology*, *7*, 10. https://doi.org/10.3389/fmicb.2016.00214

Gupta, V., Smemo, K. A., Yavitt, J. B., Fowle, D., Branfireun, B., & Basiliko, N. (2013). Stable isotopes reveal widespread anaerobic methane oxidation across latitude and peatland type. *Environmental Science & Technology*, *47*(15), 8273–8279. https://doi.org/10.1021/es400484t

Happell, J. D., & Chanton, J. P. (1993). Carbon remineralization in a North Florida swamp forest: Effects of water level on the pathways and rates of soil organic matter decomposition. *Global Biogeochemical Cycles*, *7*, 475–490. https://doi.org/10.1029/93GB00876

Hatala, J. A., Detto, M., Sonnentag, O., Deverel, S. J., Verfaillie, J., & Baldocchi, D. D. (2012). Greenhouse gas (CO_2, CH_4, H_2O) fluxes from drained and flooded agricultural peatlands in the Sacramento-San Joaquin Delta. *Agriculture Ecosystems & Environment*, *150*, 1–18. https://doi.org/10.1016/j.agee.2012.01.009

Hodgkins, S. B., Chanton, J. P., Langford, L. C., McCalley, C. K., Saleska, S. R., Rich, V. I., … Cooper, W. T. (2015). Soil incubations reproduce field methane dynamics in a subarctic wetland. *Biogeochemistry*, *126*(1–2), 241–249. https://doi.org/10.1007/s10533-015-0142-z

Hornibrook, E. (1997). Spatial distribution of microbial methane production pathways in temperate zone wetland soils: Stable carbon and hydrogen isotope evidence. *Geochimica et Cosmochimica Acta*, *61*, 745–753. https://doi.org/10.1016/S0016-7037(96)00368-7

Hornibrook, E. R. C., Bowes, H. L., Culbert, A., & Gallego-Sala, A. V. (2009). Methanotrophy potential versus methane supply by pore water diffusion in peatlands. *Biogeosciences*, *6*(8), 1491–1504. https://doi.org/10.5194/bg-6-1491-2009

Kettunen, A., Kaitala, V., Lehtinen, A., Lohila, A., Alm, J., Silvola, J., & Martikainen, P. J. (1999). Methane production and oxidation potentials in relation to water table fluctuations in two boreal mires. *Soil Biology and Biochemistry*, *31*(12), 1741–1749. https://doi.org/10.1016/S0038-0717(99)00093-0

Knoblauch, C., Spott, O., Evgrafova, S., Kutzbach, L., & Pfeiffer, E. M. (2015). Regulation of methane production, oxidation, and emission by vascular plants and bryophytes in ponds of the northeast Siberian polygonal tundra. *Journal of Geophysical Research: Biogeosciences*, *120*, 2525–2541. https://doi.org/10.1002/2015JG003053

Knorr, K. H., & Blodau, C. (2009). Impact of experimental drought and rewetting on redox transformations and methanogenesis in mesocosms of a northern fen soil. *Soil Biology and Biochemistry*, *41*(6), 1187–1198. https://doi.org/10.1016/j.soilbio.2009.02.030

Knox, S. H., Sturtevant, C., Matthes, J. H., Koteen, L., Verfaillie, J., & Baldocchi, D. (2015). Agricultural peatland restoration: Effects of land-use change on greenhouse gas (CO_2 and CH_4) fluxes in the Sacramento-San Joaquin Delta. *Global Change Biology*, *21*(2), 750–765. https://doi.org/10.1111/gcb.12745

Koh, L. P., Miettinen, J., Liew, S. C., & Ghazoul, J. (2011). Remotely sensed evidence of tropical peatland conversion to oil palm. *Proceedings of the National Academy of Sciences of the United States of America*, *108*(12), 5127–5132. https://doi.org/10.1073/pnas.1018776108

Langeveld, C. A., Segers, R., Dirks, B. O. M., van den Polvan Dasselaar, A., Velthof, G. L., & Hensen, A. (1997). Emissions of CO_2, CH_4 and N_2O from pasture on drained peat soils in the Netherlands. *European Journal of Agronomy*, *7*(1–3), 35–42.

Li, W., Dickinson, R. E., Fu, R., Niu, G.-Y., Yang, Z.-L., & Canadell, J. G. (2007). Future precipitation changes and their implications for tropical peatlands. *Geophysical Research Letters*, *34*, L01403. https://doi.org/10.1029/2006GL028364

Limpens, J., Berendse, F., Blodau, C., Canadell, J. G., Freeman, C., Holden, J., … Schaepman-Strub, G. (2008a). Peatlands and the carbon cycle: From local processes to global implications a synthesis (vol 5, p. 1475, 2008). *Biogeosciences*, *5*(6), 1739–1739.

Limpens, J., Berendse, F., Blodau, C., Canadell, J. G., Freeman, C., Holden, J., … Schaepman-Strub, G. (2008b). Peatlands and the carbon cycle: From local processes to global implications—A synthesis. *Biogeosciences*, *5*(5), 1475–1491.

Liptzin, D., & Silver, W. L. (2009). Effects of carbon additions on iron reduction and phosphorus availability in a humid tropical forest soil. *Soil Biology and Biochemistry*, *41*(8), 1696–1702. https://doi.org/10.1016/j.soilbio.2009.05.013

Lovley, D. R. (1987). Organic matter mineralization with the reduction of ferric iron: A review. *Geomicrobiology Journal*, *5*(3–4), 375–399. https://doi.org/10.1080/01490458709385975

Lovley, D. R., & Phillips, E. J. P. (1986a). Organic matter mineralization with reduction of ferric iron in anaerobic sediments. *Applied and Environmental Microbiology*, *51*(4), 683–689.

Lovley, D. R., & Phillips, E. J. P. (1986b). Availability of ferric iron for microbial reduction in bottom sediments of the freshwater tidal Potomac River. *Applied and Environmental Microbiology*, *52*(4), 751–757.

Lovley, D. R., & Phillips, E. J. P. (1987). Competitive mechanisms for inhibition of sulfate reduction and methane production in the zone of ferric iron reduction in sediments. *Applied and Environmental Microbiology*, *53*(11), 2636–2641.

Lueders, T., & Friedrich, M. (2000). Archaeal population dynamics during sequential reduction processes in rice field soil. *Applied and Environmental Microbiology*, *66*(7), 2732–2742. https://doi.org/10.1128/AEM.66.7.2732-2742.2000

Luton, P. E., Wayne, J. M., Sharp, R. J., & Riley, P. W. (2002). The *mcrA* gene as an alternative to 16S rRNA in the phylogenetic analysis of methanogen populations in landfill. *Microbiology*, *148*, 3521–3530. https://doi.org/10.1099/00221287-148-11-3521

Maljanen, M., Sigurdsson, B. D., Guomundsson, J., Oskarsson, H., Huttunen, J. T., & Martikainen, P. J. (2010). Greenhouse gas balances of managed peatlands in the Nordic countries—Present knowledge and gaps. *Biogeosciences*, *7*(9), 2711–2738. https://doi.org/10.5194/bg-7-2711-2010

Mayer, H. P., & Conrad, R. (1990). Factors influencing the population of methanogenic bacteria and the initiation of methane production upon flooding of paddy soil. *FEMS Microbiology Ecology*, *73*(2), 103–111. https://doi.org/10.1111/j.1574-6968.1990.tb03930.x

McNicol, G., & Silver, W. L. (2015). Non-linear response of carbon dioxide and methane emissions to oxygen availability in a drained histosol. *Biogeochemistry*, *123*(1–2), 299–306. https://doi.org/10.1007/s10533-015-0075-6

Megonigal, J. P., Hines, M., & Visscher, P. (2004). Anaerobic metabolism: Linkages to trace gases and aerobic processes. In W. Schlesinger (Ed.), *Biogeochemistry* (pp. 317–424). Oxford: Elsevier-Pergamon.

Miller, K. E., Lai, C.-T., Friedman, E. S., Angenent, L. T., & Lipson, D. A. (2015). Methane suppression by iron and humic acids in soils of the Arctic Coastal Plain. *Soil Biology and Biochemistry*, *83*, 176–183. https://doi.org/10.1016/j.soilbio.2015.01.022

Moore, T. R., & Dalva, M. (1993). The influence of temperature and water table position on carbon dioxide and methane emissions from laboratory columns of peatland soils. *Journal of Soil Science*, *44*(4), 651–664. https://doi.org/10.1111/j.1365-2389.1993.tb02330.x

Nesbit, S. P., & Breitenbeck, G. A. (1992). A laboratory study of factors influencing methane uptake by soils. *Agriculture Ecosystems and Environment*, *41*(1), 39–54. https://doi.org/10.1016/0167-8809(92)90178-E

Neubauer, S. C., & Megonigal, J. P. (2015). Moving beyond global warming potentials to quantify the climatic role of ecosystems. *Ecosystems*, *18*(6), 1000–1013. https://doi.org/10.1007/s10021-015-9879-4

Neufeld, J. D., Vohra, J., Dumont, M. G., Lueders, T., Manefield, M., Friedrich, M. W., & Murrell, J. C. (2007). DNA stable-isotope probing. *Nature Protocols*, *2*(4), 860–866. https://doi.org/10.1038/nprot.2007.109

Nykanen, H., Alm, J., Lang, K., Silvola, J., & Martikainen, P. J. (1995). Emissions of CH_4, N_2O and CO_2 from a virgin fen and a fen drained for grassland in Finland. *Journal of Biogeography*, *22*(2–3), 351–357.

Parkin, T. B. (1987). Soil microsites as a source of denitrification variability. *Soil Science Society of America Journal*, *51*(5), 1194–1199. https://doi.org/10.2136/sssaj1987.03615995005100050019x

Peters, V., & Conrad, R. (1996). Sequential reduction processes and initiation of CH_4 production upon flooding of oxic upland soils. *Soil Biology and Biochemistry*, *28*(3), 371–382. https://doi.org/10.1016/0038-0717(95)00146-8

Popp, T. J., Chanton, J. P., Whiting, G. J., & Grant, N. (2000). Evaluation of methane oxidation in the rhizosphere of a Carex dominated fen in north central Alberta, Canada. *Biogeochemistry*, *51*(3), 259–281.

Raghoebarsing, A. A., Pol, A., van de Pas-Schoonen, K. T., Smolders, A. J. P., Ettwig, K. F., Rijpstra, W. I. C., … Strous, M. (2006). A microbial consortium couples anaerobic methane oxidation to denitrification. *Nature*, *440*(7086), 918–921. https://doi.org/10.1038/nature04617

Reiche, M., Torburg, G., & Kuesel, K. (2008). Competition of Fe(III) reduction and methanogenesis in an acidic fen. *FEMS Microbiology Ecology*, *65*(1), 88–101. https://doi.org/10.1111/j.1574-6941.2008.00523.x

Riley, W. J., Subin, Z. M., Lawrence, D. M., Swenson, S. C., Torn, M. S., Meng, L., … Hess, P. (2011). Barriers to predicting changes in global terrestrial methane fluxes: Analyses using CLM4Me, a methane biogeochemistry model integrated in CESM. *Biogeosciences*, *8*(7), 1925–1953. https://doi.org/10.5194/bg-8-1925-2011

Roden, E. E., & Wetzel, R. G. (2003). Competition between Fe(III)-reducing and methanogenic bacteria for acetate in iron-rich freshwater sediments. *Microbial Ecology*, *45*(3), 252–258. https://doi.org/10.1007/s00248-002-1037-9

Roulet, N., Moore, T., Bubier, J., & Lafleur, P. (1992). Northern fens: Methane flux and climatic change. *Tellus Series B: Chemical and Physical Meteorology*, *44*(2), 100–105. https://doi.org/10.1034/j.1600-0889.1992.t01-1-00002.x

Roulet, N. T., Ash, R., Quinton, W., & Moore, T. (1993). Methane flux from drained northern peatlands: Effect of a persistent water table lowering on flux. *Global Biogeochemical Cycles*, *7*, 749–769. https://doi.org/10.1029/93GB01931

Schrier-Uijl, A. P., Kroon, P. S., Leffelaar, P. A., van Huissteden, J. C., Berendse, F., & Veenendaal, E. M. (2010). Methane emissions in two drained peat agro-ecosystems with high and low agricultural intensity. *Plant and Soil*, *329*(1–2), 509–520. https://doi.org/10.1007/s11104-009-0180-1

Sexstone, A. J., Revsbech, N. P., Parkin, T. B., & Tiedje, J. M. (1985). Direct measurement of oxygen profiles and denitrification rates in soil aggregates. *Soil Science Society of America Journal*, *49*(3), 645–651. https://doi.org/10.2136/sssaj1985.03615995004900030024x

Sey, B. K., Manceur, A. M., Whalen, J. K., Gregorich, E. G., & Rochette, P. (2008). Small-scale heterogeneity in carbon dioxide, nitrous oxide and methane production from aggregates of a cultivated sandy-loam soil. *Soil Biology and Biochemistry*, *40*(9), 2468–2473. https://doi.org/10.1016/j.soilbio.2008.05.012

Shannon, R. D., White, J. R., Lawson, J. E., & Gilmour, B. S. (1996). Methane efflux from emergent vegetation in peatlands. *Journal of Ecology*, *84*(2), 239–246.

Silver, W. L., Liptzin, D., & Almaraz, M. (2013). Soil redox dynamics and biogeochemistry along a tropical elevation gradient. *Ecological Bulletins*, *4*, 195–209.

Silver, W. L., Lugo, A. E., & Keller, M. (1999). Soil oxygen availability and biogeochemistry along rainfall and topographic gradients in upland wet tropical forest soils. *Biogeochemistry*, *44*(3), 301–328.

Smemo, K. A., & Yavitt, J. B. (2007). Evidence for anaerobic CH_4 oxidation in freshwater peatlands. *Geomicrobiology Journal*, *24*(7–8), 583–597. https://doi.org/10.1080/01490450701672083

Smemo, K. A., & Yavitt, J. B. (2011). Anaerobic oxidation of methane: An underappreciated aspect of methane cycling in peatland ecosystems? *Biogeosciences*, *8*(3), 779–793. https://doi.org/10.5194/bg-8-779-2011

Sonnentag, O., Detto, M., Vargas, R., Ryu, Y., Runkle, B. R. K., Kelly, M., & Baldocchi, D. D. (2011). Tracking the structural and functional development of a perennial pepperweed (*Lepidium latifolium* L.) infestation using a multi-year archive of webcam imagery and eddy covariance measurements. *Agricultural and Forest Meteorology*, *151*(7), 916–926. https://doi.org/10.1016/j.agrformet.2011.02.011

Teh, Y. A., & Silver, W. L. (2006). Effects of soil structure destruction on methane production and carbon partitioning between methanogenic pathways in tropical rain forest soils. *Journal of Geophysical Research: Biogeosciences*, *111*, G01003. https://doi.org/10.1029/2005JG000020

Teh, Y. A., Dubinsky, E. A., Silver, W. L., & Carlson, C. M. (2008). Suppression of methanogenesis by dissimilatory Fe(III)-reducing bacteria in tropical rain forest soils: Implications for ecosystem methane flux. *Global Change Biology*, *14*(2), 413–422. https://doi.org/10.1111/j.1365-2486.2007.01487.x

Teh, Y. A., Silver, W. L., & Conrad, M. E. (2005). Oxygen effects on methane production and oxidation in humid tropical forest soils. *Global Change Biology*, *11*, 1283–1297. https://doi.org/10.1111/j.1365-2486.2005.00983.x

Teh, Y. A., Silver, W. L., Sonnentag, O., Detto, M., Kelly, M., & Baldocchi, D. D. (2011). Large greenhouse gas emissions from a temperate peatland pasture. *Ecosystems*, *14*(2), 311–325. https://doi.org/10.1007/s10021-011-9411-4

Updegraff, K., Bridgham, S. D., Pastor, J., Weishampel, P., & Harth, C. (2001). Response of CO_2 and CH_4 emissions from peatlands to warming and water table manipulation. *Ecological Applications*, *11*(2), 311–326. https://doi.org/10.1890/1051-0761(2001)011[0311:ROCACE]2.0.CO;2

Valenzuela, E. I., Prieto-Davo, A., Lopez-Lozano, N. E., Hernandez-Eligio, A., Vega-Alvarado, L., Juarez, K., … Cervantes, F. J. (2017). Anaerobic methane oxidation driven by microbial reduction of natural organic matter in a tropical wetland. *Applied and Environmental Microbiology*, *83*(11), 15. https://doi.org/10.1128/AEM.00645-17

van Bodegom, P. M., Scholten, J. C. M., & Stams, A. J. M. (2004). Direct inhibition of methanogenesis by ferric iron. *FEMS Microbiology Ecology*, *49*(2), 261–268. https://doi.org/10.1016/j.femsec.2004.03.017

van den Pol-Van Dasselaar, A., van Beusichem, M. L., & Oenema, O. (1999). Methane emissions from wet grasslands on peat soil in a nature preserve. *Biogeochemistry*, *44*(2), 205–220.

von Fischer, J. C., Butters, G., Duchateau, P. C., Thelwell, R. J., & Siller, R. (2009). In situ measures of methanotroph activity in upland soils: A reaction-diffusion model and field observation of water stress. *Journal of Geophysical Research: Biogeosciences*, *114*, G01015. https://doi.org/10.1029/2008JG000731

von Fischer, J. C., & Hedin, L. O. (2002). Separating methane production and consumption with a field-based isotope pool dilution technique. *Global Biogeochemical Cycles*, *16*(3), 1034. https://doi.org/10.1029/2001GB001448

von Fischer, J. C., & Hedin, L. O. (2007). Controls on soil methane fluxes: Tests of biophysical mechanisms using stable isotope tracers. *Global Biogeochemical Cycles*, *21*, GB2007. https://doi.org/10.1029/2006GB00268

Wania, R., Melton, J. R., Hodson, E. L., Poulter, B., Ringeval, B., Spahni, R., … Kaplan, J. O. (2013). Present state of global wetland extent and wetland methane modelling: Methodology of a model inter-comparison project (WETCHIMP). *Geoscientific Model Development*, *6*(3), 617–641. https://doi.org/10.5194/gmd-6-617-2013

Whalen, S. C., & Reeburgh, W. S. (1990). Consumption of atmospheric methane by tundra soils. *Nature*, *346*(6280), 160–162. https://doi.org/10.1038/346160a0

Whipple, A. A., Grossinger, R. M., Rankin, D., Stanford, B., & Askevoid, R. A. (2012). Sacramento-San Joaquin Delta historical ecology investigation: Exploring pattern and process, (Rep.), San Francisco Estuary Institute-Aquatic Science Center, Richmond, CA.

Yang, W. H., & Silver, W. L. (2016). Net soil-atmosphere fluxes mask patterns in gross production and consumption of nitrous oxide and methane in a managed ecosystem. *Biogeosciences*, *13*, 1705–1715. https://doi.org/10.5194/bg-13-1705-2016

Yang, W. H., Teh, Y. A., & Silver, W. L. (2011). A test of a field-based ^{15}N-nitrous oxide pool dilution technique to measure gross N_2O production in soil. *Global Change Biology*, *17*(12), 3577–3588. https://doi.org/10.1111/j.1365-2486.2011.02481.x

Yao, H., Conrad, R., Wassmann, R., & Neue, H. U. (1999). Effect of soil characteristics on sequential reduction and methane production in sixteen rice paddy soils from China, the Philippines, and Italy. *Biogeochemistry*, *47*(3), 269–295.

Yavitt, J. B. (2013). Recovery of methanogenesis following summer drought in soils from two cool temperate peatlands, New York State, USA. *Geomicrobiology Journal*, *30*(1), 8–16. https://doi.org/10.1080/01490451.2011.638699

Zinder, S. H. (1993). Physiological ecology of methanogens. In J. G. Ferry (Ed.), *Methanogenesis-Ecology, Physiology, Biochemistry & Genetics* (pp. 128–206). New York, London: Chapman & Hall.